HyDelta 2

WP5 – Safe operations of the high-pressure transmission grid

D5.1 – Venting and flaring

Status: final

Dit project is medegefinancierd door TKI Nieuw gas | Top Sector Energy uit de PPS-toeslag onder referentienummer TKI2022-HyDelta.

Document summary

Corresponding author

Corresponding author	Nard Vermeltfoort
Linked to	Kiwa Technology B.V.
Email address	Nard.Vermeltfoort@kiwa.com

Document history

Version	Date	Author	Summary of changes
1	12-May-2023	Nard Vermeltfoort (Kiwa), Sander Lueb (Kiwa), Néstor González Díez (TNO), Harmen Slot (TNO)	First draft version.
2	16-June-2023	Nard Vermeltfoort (Kiwa), Sander Lueb (Kiwa), Néstor González Díez (TNO), Harmen Slot (TNO)	Second draft version.
3	28-June-2023	Nard Vermeltfoort (Kiwa), Sander Lueb (Kiwa), Néstor González Díez (TNO), Harmen Slot (TNO)	Draft for Supervisory Group
4	25-July-2023	Nard Vermeltfoort (Kiwa), Sander Lueb (Kiwa), Néstor González Díez (TNO), Harmen Slot (TNO)	Final English

Distribution level

PU	Public	X
RE	Limited to • Project partners including Expert Assessment Group • External entity with whom a duty of confidentiality exists	

Document review

Partner	Name
Stedin	Gilles de Kok
Gasunie	Martin van Agteren
Gasunie	Martin Hommes
DNV	Pieter Wolff
NBNL, Gasunie, Kiwa, DNV, TNO, NEC, Hanze	HyDelta Supervisory Group

Summary

As part of the national research programme HyDelta, a study was carried out into the possibilities of depressurising high-pressure hydrogen transport pipelines by venting and flaring. The research as described in this report is part of work package 5 "Working safely on the high-pressure transport network".

Gasunie was commissioned by the Dutch government to create a national hydrogen transport system. During the operation of this network sometimes modifications have to be made to this transport system. In some cases hydrogen needs to be extracted from the network in a controlled manner to be able to work safely. To decrease the amount of hydrogen that has to be extracted, this will be done by pressure equalisation and followed by recompression. The residual hydrogen in the transport network has to be removed via venting or flaring.

To determine whether high-pressure hydrogen pipelines can be depressurised using venting and flaring, 13 more specific research questions were formulated. These were answered by conducting theoretical and practical research.

The theoretical study considered the differences between venting and flaring in general and made a comparison between flaring of natural gas and hydrogen. In addition, market information was gathered by interviewing two large industrial users familiar with hydrogen flaring and two flare installation suppliers.

In the practical investigation, a flare was assessed for;

- Direct ignition behaviour
- The behaviour in delayed ignition
- The risk of flame impact

Various measurements were performed; flow rate, heat radiation, flame appearance, noise levels, wind speed and NOx emissions.

The findings of the experiments were compared with theory and various mathematical models. In particular, the flow profile through the flame arrestor, flame height, heat radiation and noise production were compared.

The overall conclusion is that flaring is preferable instead of venting. This is after pressure equalisation and recompression has taken place. With the utilized flare installation, flaring of flow rates of 500, 2500, 4000 and 6000 Nm^3/h were possible. During the experiments, no excessive noise production or excesses in pressure waves were observed. It is recommended to validate to what extent the results can be extrapolated for the application of flaring of larger flow rates and at larger diameters.

In any hydrogen combustion process, forming NOx can be an issue. It is recommended to carry out further research on NOx measurements and reducing measures. For the design of hydrogen flare plants, existing theoretical models can be used. The results obtained from the experiments appear to be in reasonable agreement with the theoretical findings.

Content

1. Introduction

1.1 General

This research was conducted as part of the national research programme HyDelta. This programme focuses on the safe incorporation of hydrogen into the existing gas transport and distribution infrastructure and aims to remove barriers to innovative hydrogen projects. The full research programme is divided into work packages. For an explanation of the different work packages, see www.hydelta.nl .

1.2 Problem statement

Gasunie has been commissioned to create a national hydrogen transport system. During the operation of this network, adjustments and/or extensions sometimes have to be made to this transport system. For safety reasons, in some cases hydrogen needs to be extracted from the network in a controlled manner. The option with the lowest gas emissions would be by first levelling (or lowering) the pressure (buffering out) and then recompressing the remaining hydrogen. However, recompression does not allow a pipeline to be completely H_2 -free: the last part of residual hydrogen needs to be vented or flared. This is comparable with the currently used method for natural gas.
In this work package, the methods are first considered theoretically. The experimental studies focused on flaring; it emerged at the start of the study that flaring is preferable instead of venting because of the indirect greenhouse gas effect of H_2. Flaring is also preferred over venting for safety reasons: if a hydrogen gas cloud ignites unexpectedly during venting, the consequences can be much greater than for a natural gas cloud, due to the higher flame velocity of hydrogen. According to current Gasunie procedures for natural gas, the nominal working pressure can be reduced from 67 barg to 7 barg via recompression. In this study, the assumption is that these pressures also apply to the future hydrogen transport system. Flaring will take place at the pressure of 7 barg. Flaring at a pressure of 7 barg corresponds to the highest pressures at which regional network operators will flare. In the high-pressure pipeline system of the regional network operators, there is a maximum pressure of 8 barg. Before regional grid operators start flaring hydrogen in their high-pressure distribution pipelines, they will first reduce the pressure via demand from the low-pressure grid. In any case, the results in this report are applicable to flaring with pressures < 8 barg.
This report describes the experimental tests carried out, and the results obtained. It also describes models that are useful for making predictions regarding flaring. These models can be used to simulate new flare installations so that their operation at larger flow rates can be investigated before being tested in practice.

1.3 Objective

Determine how to safely depressurise high-pressure hydrogen transport pipelines by means of venting and primary flaring. This is based on the premise that the high pressure is reduced as much as possible prior to flaring by, for example, extraction and recompression.

1.4 More specific research questions

To meet the aforementioned objective, specific research questions have been formulated. These research questions are as follows;

- What (industry) standards are available for venting and flaring?
- Are hydrogen flare systems for sale?
- What are the differences with natural gas in terms of venting and flaring?
- What are the principles of safety?
- What is the thermal radiation of a flare for hydrogen?
- What is the maximum pressure in the flare installation?
- What happens to the burner? What will be the size of the flame?
- Can hydrogen be ignited at the different flow rates/velocities?
- What is the effect of delayed ignition?
- Can detonation occur with delayed ignition? (theoretical consideration)
- Can unwanted ignition occur when venting? (e.g. from electrical discharge or friction due to high speeds)
- What are the effects of flaring if the pipeline is almost empty?
- What NOx emissions occur?

The experiments were carried out at the Twente Safety Campus (TSC). At that time, Gasunie was working on another project that could be combined with these flare tests.

2. Venting and flaring

2.1 Introduction

The increasing scale of hydrogen adoption as an energy carrier leads to the need to transport hydrogen over long distances from production to end users. This is the case, for example, of large-scale offshore wind farms connected to power-to-gas plants, which send the produced hydrogen to the coast; or international transport from countries developing large renewable electricity generation capacity to countries with high industrial demand. To transport hydrogen via pipelines over long distances, a transport system based on high pressure usually proves to be the most economical, as is the case for the transport of natural gas [1].

In the operation of such high-pressure (hydrogen) pipeline systems, it may be necessary to be able to quickly reduce the pressure in a particular (bounded) segment of the system. This may be necessary in emergency situations or during planned maintenance. In the simplest solution, typical of most systems, the segment of the system to be relieved is bounded with valves or other equipment. The isolated volume is either vented to the environment or flared, if recompression is not available or possible. For transmission systems, flaring is always preferred to blowdown because of the potential of natural gas as a greenhouse gas. System operators use recompression to route gas from the isolated segment of the transmission system to a neighbouring segment. Re-compression equipment consists of a small compressor mounted on a trailer that can be taken to different segments of the network. Applying recompression means minimal environmental damage is caused and no valuable product is lost. Of course, this is only possible when depressurisation is part of a planned activity.

As hydrogen recompression equipment is currently commercially unavailable or of limited availability, and is also not sufficient to depressurise the entire system, pressure reduction must be performed by either blowdown or flaring. In both cases, a temporary mobile plant is used. It is not self-evident that, as for natural gas, hydrogen is better flared than blown off. Flaring also involves risks that cannot compensate for possible environmental benefits. Until very recently, studies paid little attention to the potential of hydrogen as a greenhouse gas. Recent literature [2] indicates that hydrogen does have an impact as an indirect greenhouse gas. The best option between flaring and blowdown may depend heavily on local conditions. In general, the following perspectives should be explored:

- Safety: the wide flammability range of hydrogen combined with its low ignition energy creates risks for delayed or unintended ignition during blowdown. The blown-off hydrogen from a high-pressure system will rapidly diffuse and form flammable mixtures with atmospheric air, which can lead to catastrophic accidents if an ignition source is present. Flaring is also not free of safety risks, although it is a controlled process. The operation must be monitored and personnel must be at a safe enough distance to protect themselves from radiation heat.
- Environmental impacts: burnt hydrogen in a flare will mainly produce water vapour, but due to the high flame temperature it is also more prone to form nitrogen oxides. It has recently been shown that blown-off hydrogen carries indirect global warming potential.
- Regulatory condition: the operation must be carried out in compliance with local regulations in the context of environment, safety and with regard to disruption to the community around the site of the blowdown or flare plant.

The current prevailing view is that, as hydrogen can help reduce fossil fuel use in the energy sector, flaring is preferable to blowdown to achieve the intended minimum emissions of CO_2.

2.2 Flaring

In the context of hydrogen production in industry, hydrogen flaring is the controlled combustion of hydrogen gas under atmospheric conditions by means of dedicated flaring plants. Controlled hydrogen combustion can occur in processes where hydrogen is produced as a by-product of oil and gas production, refining or other chemical production processes. Hydrogen flaring already occurs in the context of industrial plants. The operation can be performed for mixtures of hydrogen with other gases or for near-pure hydrogen[1] . How the flaring operation can be performed is determined by standards covering four main areas:

- Environmental regulations: these rules may set limits on the amount of hydrogen that may be flared in case pollutants are formed, as well as the duration and frequency of flaring.
- Occupational health and safety standards: there may be standards to protect workers from hazards arising from the operation, such as increased noise or heat radiation.
- Energy efficiency standards: flaring is not a very efficient way of disposing of excess gas, as it results in the loss of a valuable energy source. Some countries have implemented standards to encourage the use of more efficient methods of waste disposal, such as capturing and reusing the gas or converting it into electricity.
- Industry-specific standards: there are also industry-specific standards applicable to hydrogen flaring. For example, the oil and gas industry has standards related to flaring that are specific to that industry.

Standards that can be applied to hydrogen flaring are shown in Table 1

Table 1: List of standards that can be applied to hydrogen flaring.

Standard	Title	Edition	Region
API 521	Pressure-Relieving and Depressuring Systems	2020	USA
ASME B31.12	Hydrogen Piping and Pipelines	2020	USA
EIGA 121	Hydrogen Pipeline Systems	2014	Europe
EIGA 15	Gaseous Hydrogen Installations	2021	Europe
EIGA 211	Hydrogen Vent Systems for Customer Applications	2017	Europe
NFPA 55	Standard for the Storage, Use, and Handling of Compressed Gases and Cryogenic Fluids in Portable and Stationary Containers, Cylinders, and Tanks	2023	USA

2.3 Comparison between hydrogen and natural gas flaring

Generally, the gases to be burned are brought to a remote location, sometimes in an elevated position, and burned in a flame using a specially designed burner tip. Sometimes certain gases are injected to promote mixing efficiency. The combustion process can only be started when three elements are present: 1) a fuel, 2) an oxidant and 3) an ignition source. However, the fuel component must meet a concentration requirement: if the concentration of the fuel is too low (i.e. below the lower flammability limit), no combustion will take place. Similarly, if the fuel mixture is too rich (i.e. the concentration of the fuel is higher than the upper flammability limit), no combustion will take place. Combustion in a flare is a turbulent process. Undesirable side effects include (heat) radiation,

[1] In the context of this report, pure hydrogen is assumed to be representative of the hydrogen that will flow in hydrogen pipeline transportation networks.

noise, and emissions of NOx/CO. These effects can be reduced by proper flare and flare process design.

This paragraph details the main differences between the flare process of hydrogen and natural gas, and how these differences require flare design modifications. Table 2 lists some properties of natural gas and hydrogen that are relevant to flaring.

Table 2: Brief overview of Table 2 properties of natural gas and hydrogen related to flaring.

Property	Natural Gas	Hydrogen	Unit
Density (normal conditions)	0.72	0.09	kg/m^3
Diffusion coefficient	0.016	0.061	m/s^2
Flame speed	0.4	1.7-3.5	m/s
Flame temperature	1937	2182	˚C
Combustion value (H*i*, normal conditions)	31.65	10.8	MJ/Nm^3
Stoichiometric air requirement	0.31	0.24	kg/MJ
Visibility	Visible - Blue/yellow flame	Visible in infra-red	
Emissions	CO, H_2O and trace constituents	H_2O and N_2 ; risk of NO_X production	
Sound		The noise produced is significantly greater compared to natural gas, due to the high exhaust velocity. The noise produced has a high frequency.	

From Table 2 we can see from the values of (bulk) density (at atmospheric conditions) and diffusion coefficient that hydrogen will expand faster in a given volume compared to natural gas. Due to the lower density of hydrogen, at a given pressure and burner geometry, the resulting volume flow will be about 3 times higher compared to that of natural gas.

A typical burner design includes several components and a refractory throat or tile. The increased flame temperature of hydrogen compared to that of natural gas requires increased quality of the steel (or other applied metal) used to construct the nozzle, throat and flame stabilizers to a higher-grade stainless steel or alloy variety. The steel used in burners that burn hydrogen should not be susceptible to hydrogen embrittlement and to hydrogen degradation at high temperatures. Both phenomena can degrade an incorrectly chosen steel prematurely, leading to premature failure of burner components.

Combustion processes using air with a flame temperature above T=1371 °C, are prone to the formation of nitrogen oxides (NO_X) due to the reaction of N_2 with O_2. The increased combustion speed of hydrogen therefore has an increased risk of NO_X formation compared to natural gas combustion.

Table 2 shows that hydrogen has a significantly higher flame velocity compared to natural gas. This means that if the volume flow of air and hydrogen to the combustion area is lower than the combustion rate, the combustion area will be closer to the flame tip. In premixed flare applications, there is therefore a risk of flame penetration into the flare column if the exit velocity of the fuel/air

mixture is too low. This can be prevented by switching to a non-premixed application (e.g. a diffusion flare) or by keeping the exhaust velocity sufficiently high by reducing the nozzle exit diameter or maintaining it above a minimum pressure. For premixed flare designs, it is necessary to implement risk mitigation measures to prevent the flame from reaching the connected process piping. This is usually done by means of a flame arrestor. It is important to note that even for diffusion-type flares, it is good practice to install a flame arrestor to protect the connected process piping from unforeseen processes where a flame may propagate to the process piping.

Another important difference between hydrogen and natural gas is that hydrogen can be susceptible to ignition by static electricity, possibly due to electrostatic discharges at the sharp edge of the outlet orifice or chemical reaction between hydrogen and FeO particles. According to API 521, such electrostatic discharges can be prevented by installing a toroidal ring on the flare tip.

2.4 Market research

Interviews were held with various market players to determine the state of flare equipment on a relevant scale. In particular, interviews were held with suppliers of mobile flare equipment on the one hand, but also with petrochemical and industrial parties that are expected to flare hydrogen (of high purity) in their processes (if required). A total of 8 parties were approached, of which 2 from the large-scale industry and 2 flare suppliers were open to interview.

All parties interviewed highlighted different aspects:

- Existing technical guidelines provide a framework for hydrogen flaring;
- Specific aspects of flare design for hydrogen: the role of the flame arrestor (or other sealing device) in combination with the available pressure is an important safety aspect;
- Flaring is preferable to blow-off.

Some notes from each of the interviews are given below:

Large-scale industrial user 1

- Use a lockout-tagout (LOTO) procedure to check the leak tightness of gate valves before flaring the segments to be degassed.
- One of the main concerns is the possibility of flame flashback during hydrogen flaring. In the flare system, a water-filled separator vessel is used to prevent contact between oxygen and hydrogen before flaring, as described in API 521.
- Hydrogen flaring is preferred, as uncontrolled ignition due to buoyancy and diffusion is not desirable. Hydrogen flaring is therefore not considered.
- There are no knowledge gaps to design a suitable flare for hydrogen applications. Standards are available and the market is ready to meet this need.

Large-scale industrial user 2

- It is very likely that if venting (cold flare) takes place, a flame will still be created (e.g. due to Joule-Thomson heating), therefore flaring is preferred. Venting hydrogen will almost certainly lead to ignition with an accompanying bang. The flame will extinguish if the exhaust velocity of hydrogen is sufficiently high.
- Hydrogen flows quickly and burns at high temperatures, so expect increased noise production and heat radiation as a result.
- Hydrogen flaring is considered relatively safe and standard modelling is adequate. For example, guidelines regarding thermal radiation from flares can be found in reference [3].

Key design parameters for a flare system (sizing, noise) can be calculated with existing models without using CFD.
- Flares will be placed in a high position, with 6 metres not unusual. Mobile flares are usually cold flares, organising hot flares is difficult (depending on the location). People's exposure to heat radiation determines the distances for staff and the public around the flare.
- A flare as intended for natural gas can also be used for hydrogen, but modifications are required. Modifications include the use of a backpressure regulator, the application of a flame arrestor, the removal of any premixing and modification of the tip of the burner.
- Depending on the country, temporary flares (e.g. up to 200 hours of use) are not regulated. Permanent flares are.

Supplier 1

- Hydrogen flaring occurs mainly in the chemical industry and is currently not a common practice in (high-pressure) transmission pipeline systems.
- In principle, it is possible to use a non-premixed flare system designed for natural gas applications for hydrogen flaring, but there is a limitation in the form of a required minimum floating pressure differential; a lower exhaust velocity creates air intake, which increases the risk of flame backfire. You also need a flame arrestor and even a detonation damper in case a pressure wave propagates into the flare system.
- Heat impact is low and heat radiation is more limited, hydrogen burns quickly and makes a lot of noise.
- The flame is not visible - in the past, animals have been injured because they could not see the flame. UV or IR cameras are needed to check the status of the flame.
- Enclosed flares are preferred for environmental reasons: the process in the internal volume is controlled and noise is blocked.

Supplier 2

- Hydrogen flaring is considered a special operation requiring safety considerations.
- Mobile flares in use [in the country where the supplier is located], closed flames are preferred due to emission regulations. Air inflow is controlled by temperature measurement in the flame zone. Insulation with ceramic materials is used to retain heat.
- A large flare capable of 3000 Nm^3/h can be 3 metres wide, 10 metres high and weigh 4 tonnes. It is difficult to make this mobile.
- Using the flare as an "open flare" is only allowed for emergency situations, up to 200 hours per year.
- A flame arrestor is necessary, but it is a rather expensive component. This solution is preferable to the water sealing drum solution.
- Useful references for regulatory framework conditions include TA Luft (*Technische Anleitung zur Reinhaltung der Luft*) and ISO 22580.

Summary

In summary, the following observations were made based on these interviews:

- Design: there is sufficient knowledge to design a flare suitable for high-purity hydrogen. Existing models or technical standards can be used for this purpose. Special attention should be paid to hydrogen with the inclusion of a flame arrestor in the flare column. A second observation is the preference for enclosed flares, in some cases open flares may only be used for temporary operations up to 200 hours, depending on local regulations. There may be

opportunities to reuse natural gas flares for hydrogen, although no clear statement on this has been received.

- Operation phase: it is best to flare compared to vent. Flaring is safer in terms of preventing uncontrolled ignitions and it is more environmentally friendly (because of the potential indirect greenhouse gas emission from hydrogen). Safety for personnel and the public should be considered with regard to heat radiation and noise considerations.
- Market readiness: none of the parties consulted had experience with mobile flares for increased hydrogen flow rates, only stationary and small applications.

2.5 NOx emissions at flare plants

Natural gas flaring will release some NOx in addition to CO_2. When hydrogen is flared, no CO_2 is released, but there is a chance on increased NOx emissions. NOx can be harmful to humans because it can cause respiratory complaints. NOx also precipitates in nature, reducing biodiversity.

For gas fired installations, the Dutch government has set emission requirements through the “Activiteitenbesluit Emissie-eisen stookinstallaties” (ABees). These emission requirements depend on the type of gas installation, the thermal power input, the type of fuel, the operating time and also the moment of commissioning. For a flare installation that burns natural gas or hydrogen and where the heat is not recovered, there are no NOx emission requirements. This is regardless of the operating time. For example, for a boiler < 50 MW, fired with natural gas and more than 500 operating hours per year, ABees states a requirement for NOx of 70 mg/Nm^3 at 3 vol% O_2 (this corresponds to 35 ppm). If the operating time of the same boiler is less than 500 hours per year then this NOx requirement no longer applies.

In the HyDelta report "Literature research on low NOx hydrogen burners and developing design rules for low NOx burners" [4] the effect on NOx emissions in the case of hydrogen combustion in mainly industrial combustion plants was named and techniques to counteract increases in NOx emissions were identified. NOx emissions at flare plants are not described in this report. In this report, a value of 600 ppm is reported for a burner in a glass-melting furnace in case of 100% hydrogen.

3. Method and description of the experimental setup

3.1 Methodology of the experiments conducted

For venting and flaring, it was originally planned to use a converted natural gas flare installation from the Gasunie. This option could not be used because the proposed conversion was not considered safe by Gasunie. It was decided to use a venting or flare installation as currently on the market. This flare installation was developed specifically for hydrogen flaring, particularly because of the presence of a flame arrestor.

In the recent past, two studies were conducted that also considered hydrogen flaring. Compared to these two conducted studies (Kiwa Technology report GT-200096 commissioned by Netbeheer Nederland and Kiwa Technology report GT-200311 commissioned by Gasunie), the experiments are innovative in the following areas:

- Larger flaring flow rates
- Quantification/measurement of thermal radiation
- NOx emission measurements
- (more extensive) delayed ignition
- Flaring hydrogen from a nearly empty pipe

In the experiments, the flow rates were varied by operating the valve at the buffer and controlling the pressure through the pressure regulators at the cylinder packs. The measurements can be divided into the categories;

- Behaviour at direct ignition
- Behaviour at delayed inflammation
- Assessment of probability of flame flashback

The direct ignition behaviour was assessed at four flow rates ranging between 700 to about 6000 Nm^3/h. The released hydrogen was ignited by the presence of a flame originating from a propane burner. This was an integral part of utilized flare installation. A total of eight measurements were performed with direct ignition of hydrogen by means of the propane burner.

The behaviour at delayed ignitions was assessed at a three flow rates ranging between 250 and 3200 Nm^3/h . The delayed ignition was applied by remotely energising a spark igniter. Reference measurements were started, i.e. opening the gas supply when the spark igniter was energised. This made it possible to determine how quickly a hydrogen cloud ignites in the relevant setup. Seven measurement series were carried out in which the flow rate and the moment of ignition remained the same for each measurement series. In a measurement series, several measurements were taken to determine the reproducibility.

The risk of flame flashback was assessed by slowly draining the gas line and buffer by closing the gas supply from the cylinder packs. This assessment was carried out three times.

3.2 Schematic representation of the measurement setup

To carry out the blowdown and flare tests, the setup was built[2] as shown in Figure 1 schematically shown.

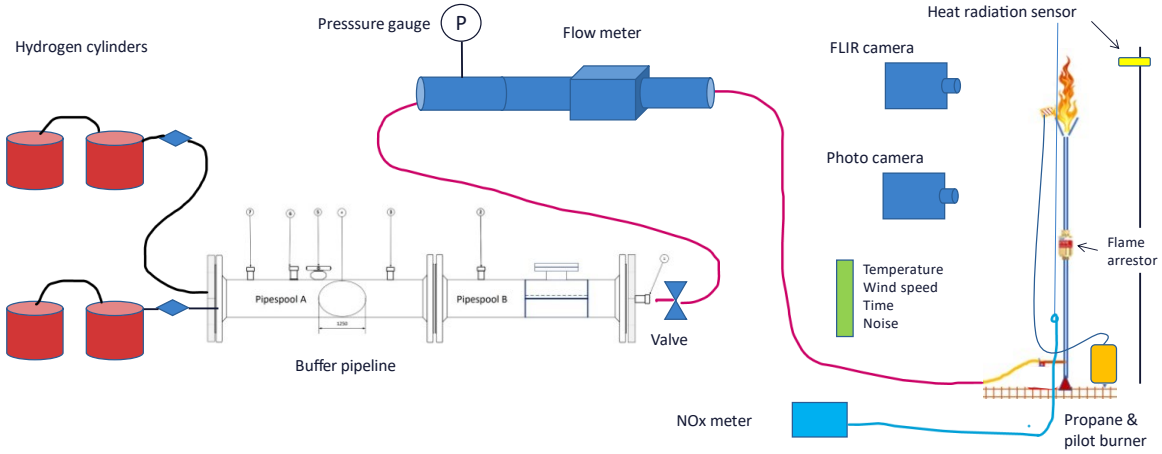

Figure 1: Schematic representation of the experimental setup.

The direction of flow in the diagram is from left to right. On the left are the cylinder packs. Connected to these were pressure regulators that could deliver a high flow rate. These had a maximum adjustable pressure of 16 bar. Other pressure regulators with a higher maximum pressure were also available, but as these could not deliver the intended flow rate, they had not been used.

If necessary, a total of 4 packages could be connected simultaneously to fill the buffer line. During testing only 1 pressure regulator was available due to circumstances, the highest flow rates were achieved with 3 connected cylinder packages. Most of the delayed ignition tests could be done with 1 package and 1 regulator.

Two pipes ran from the packages to the buffer pipeline section. This pipeline had an internal volume of 2.11 m^3 and could be filled with hydrogen up to a maximum of 68 bar. The pipeline section was used as a buffer and a valve location. Because the high-flow pressure regulator had a maximum pressure of 16 bar, the maximum pressure did not exceed 16 bar during the tests. After the valve, a 2.5" hose ran to the flow meter setup. This consisted of a pipe section with a pressure gauge, followed by a 500mm straight pipe section to even out the flow in front of the flow meter (rotor gas meter). After the flow meter, another 4" pipe section was placed. Connected to this is a 2.5" flexible hose connected to the flare installation. A built-in propane burner was used to ignite the flame or, during the delayed ignition tests, a spark generator.

[2] *The part of the measurement set-up that served as a buffer (pipespool A and pipespool B) was supplied by Gasunie and was already at the test site (Twente Safety Campus). Gasunie has in fact, through another study, not part of the HyDelta 2.0 project, investigated the extent to which welding and stopple work can be carried out safely in a hydrogen environment*.

In Figure 2 is a sketch of the top view visible. This shows the flame in the centre, and around it are the various remote measuring devices.

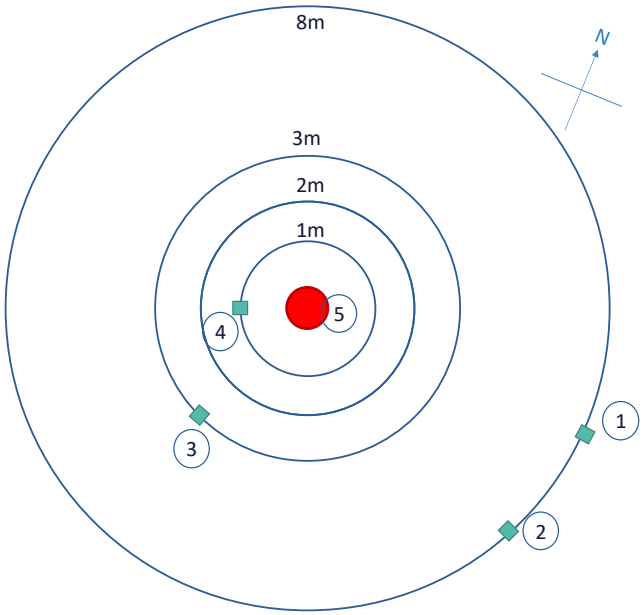

Figure 2: Sketch of the top view of the set-up

The following measuring equipment is visible:

1. The FLIR thermal imaging camera (at 1.5m height)
2. The photo camera (at 1.5m height)
3. The sound meter (at 1.3m height, at a later stage moved from 3m to 6m)
4. The thermal radiation sensor (at 1m height above the flare exit opening and at 2m distance from the exit opening (for measurement 1 and 2 at 1m distance))
5. The centre of the flare, containing the NOx intake point (1m above the outlet).

3.3 Details of the equipment used

3.3.1 The flare

The flare for these tests was provided by the company Esders. The flare installation is grounded and secured with three guy wires. The tube of the flare installation has a diameter of 2". The flare installation has Esders article number 402208. The installation is equipped as standard with a hydrogen flame arrestor of the brand Kito (type FS-Def0-IIC-2" and K215763/22), this is installed in the middle of the upright pipe (just below the securing of the guy wires, see figure 4). The flare installation is designed for the application with hydrogen but has not yet been tested with maximum flows. The flame arrestor is assumed to be the limiting factor in terms of flow restriction. According to Esders specifications, at a pressure difference across the flame arrestor of 300 mbar, a flare flow rate of 5000 Nm^3/h hydrogen would be feasible. This is stated based on conversion of air flow rate to hydrogen flow rate and extrapolation from 100 mbarg to 20 barg.
The hydrogen flowing from the chalice burner is ignited by a flame from the attached propane burner. The propane is ignited by igniter that is part of the flare system. The push button of this igniter can remain permanently energised. For the tests with the delayed ignitions, an external spark igniter was added that could be remotely energised.

Figure 3: The burner of the flare with the suction pipe of flue gases (red arrow) and Figure 4 and Figure 5 The burner of the flare with the added spark igniter (yellow arrow).

3.3.2 Flowmeter and Pressure gauge

To measure the flow rate, a rotor meter was used. The model is an Instromet SM-RI-X-L. This meter has a measurement range of 32 to 650 m^3/h with an accuracy of ± 0.2%. The maximum allowable pressure is 18.8 bar. Considering the expected pressures at the meter, the measuring range was in the desired regime. According to the inspection report, the minimum volumetric mass (density) should be between 0.5 and 18.8 kg/m^3. For hydrogen, this would mean a minimum pressure of 5.55 bar for accurate measurement. Especially in the low flow rates, this pressure was not achieved, which made the measurements in this regime less accurate. The pressure was measured using a Badotherm pressure gauge with a maximum measuring range of 16 bar and an accuracy of ±0.2 bar. Recording of both measurements was done by filming both meters in a single frame (see Figure 6).

Figure 6: Flow meter (left, yellow), Pressure gauge (right), Anemometer (top centre), Flue gas analysis reader (bottom centre) in a single frame that was recorded by a camera.

3.3.3 Sound meter

To record sound levels during the measurements, a sound meter from Brüel & Kjaer type 2250 was used. The manufacturer does not specify an accuracy margin.

Figure 7: The Bruel & Kjaer sound meter and its position in the measurement setup (yellow arrow).

During the measurements of direct ignition and assessment of flame flashback probability, the sound meter was placed at a distance of 3 metres from the flare installation. During delayed ignition, one of the last measurement series reached the maximum of the meter. At that measurement, the sound meter was then moved to a distance of 6 metres from the flare installation.

The measurements included the following parameters;

LCpeak; The maximum sound level during a measurement. L stands for Level, C stands for C-frequency. This value is used to assess possible hearing damage in people caused by short-term high noise levels.

LAFmax: The maximum sound level based on A-frequencies and a "fast time response". L stands for Level, A for A-frequency weighting factor and F for fast. It is the highest level of audible noise that occurred during the measurement time, excluding the lowest and highest frequencies.

LA eq: The average sound level based on A frequencies.

For frequency weighting factors, the additions A, C and Z are common. For Z, all frequencies are included. So both low frequencies (hums) and high frequencies (squeaks). With A, the highest and lowest frequencies are not included. With C, the highest and lowest frequencies are included in the presented value. At noise levels below 100 dB, people do not hear the low and high frequencies or hear them less well. When sound levels become high (> 100 dB), human hearing actually becomes more sensitive to both the high and low frequencies and can therefore receive even louder sounds. It is therefore common to apply A-frequency weighting for sound levels below 100 dB and C-frequency weighting for sound levels above 100dB.

3.3.4 Flue gas analyser

A flue gas analyser from ECOM type J2KN pro was used to measure NOx and oxygen concentrations in the flue gases. The flue gas sampling point took place 1 metre directly above the flare (see Figure 1 and Figure 3). Extracting all flue gases was not feasible in this arrangement. Because extraction was carried out at one point above the flare, with the measurement point sometimes being outside the flame due to the wind, NOx emissions were not measured in all cases. This does not mean that no emission of NOx took place at that time. For the measurements with delayed ignitions, no NOx measurements were made because flaring took place for a short time. The NOx emission can be determined in a range of 0 to 4000 ppm a has an accuracy of ± 5% of the reading. The accuracy of the oxygen measurement is ± 0.3% (absolute value).

Figure 8: The flue gas analyser ECOM type J2KN pro

3.3.5 Heat radiation sensor

Heat radiation was measured with a Hukseflux HF03-LI19 (see Figure 9). This consists of an HF03 sensor holder, containing the SBG01 thermal radiation sensor and an LI19 readout unit. The sensor has a measurement range of 0 to 10 x 10^3 W/m^2 . This fits into the expected range based on heat radiation calculated in other literature. The sensor can briefly measure higher values (up to 15 x 10^3 W/m^2) and is accurate by 0.1 x 10^3 W/m^2. Varying the distance from the flame ensured that the heat radiation remained within the sensor's measurement range. For the first two measurements, the distance was 1 metre. However, this overloaded the sensor and caused the connecting cable to melt. Placing the heat radiation meter another metre away from the flame solved this problem.

Figure 9: The Hukseflux LI19-HF03

3.3.6 Wind gauge

The wind meter used was a JDC Skywatch Eole, see Figure 10.

Figure 10: The JDC Skywatch Eole wind meter (Left) and the FLIR E40 (Right)

The wind meter is wind direction independent, has an accuracy of ±3% Full Scale and can measure from 2 to 150 km/h. The wind meter is positioned near the flare at a height of 1 to 2 metres. Before testing, it was set so that the average value was displayed over the past minute. This is also the value as recorded during the measurements.

3.3.7 Thermal imaging camera

The thermal imaging camera used, was of the FLIR brand and type E40. The FLIR E40 has 160 x 120 pixels, a high temperature range (up to 650 degrees Celcius) and high thermal sensitivity (<0.07°C). The accuracy is ±2°C, or ±2% Full Scale. By using this camera, the flame contour could be made visible.

4. Results of the experimental study

The measurements were carried out according to a pre-established measurement plan. While measurements were being taken, changes were made to the measurement programme. This had several reasons, e.g. the available quantity of hydrogen was limited and on-site flow rates could not be read quickly. However, by varying the pre-pressure in the pipeline, it was possible to test with different flow rates. In total, experiments were carried out on three different days. A start was made by getting the gas buffer, flare and all measuring equipment operational. On the second day, there were mainly experiments with direct ignition of different flow rates. On the third day, there were experiments with delayed ignitions and maximum flow rate tests.

4.1 Direct ignition

The direct ignition experiments were conducted by igniting the propane flame. This is the built-in ignition source during normal operation of this flare. Flames with different flow rates were tested. It started with a relatively limited pressure in the hydrogen buffer. This was used to validate the operation of the flare on hydrogen in a controlled way. These tests showed that the flare is suitable for hydrogen. No unexpected events were observed. In Table 3 are listed the direct ignition measurements performed and their corresponding flow rates.

Table 3: Direct ignition measurements performed

Meas. No.	Date	Description	Flow rate (avg) (Nm3/h)	Startpress. at spool (bar)	Startpressure at gasmeter (bar)	Windspeed (m/s)
1	06/02/2023	Experiment with low flow rate	680	2	2,0	0,2
2	06/02/2023	Experiment with low flow rate	780	2	2,0	0,3
3	07/02/2023	Emptying buffer, examination flashback	n.b.	6	2,0	0,4
4	07/02/2023	Full spool, slowely burning to empty spool, at the end 2nd examination on flash back	n.b.	6	2,0	0,4
5	07/02/2023	Increase of flowe rate by increase spool pressure	2500	8	4,2	0,8
6	07/02/2023	Increase of flowrate, incorrect measurement related to determination of flow rate	n.b.	16	10,2	0,3
7	07/02/2023	Increase of flowe rate by increase spool pressure	3750	16	8,3	0,6
8	07/02/2023	Full spool, slowely burning to empty spool, at the end 3rd examination on flash back	n.b.	8	2,5	0,5
9	09/02/2023	Maximum feasible flow rate in this set-up	n.b.	16	12,4	0,6
10	09/02/2023	Maximum feasible flow rate in this set-up	6200	16	13,0	0,3
Alle measurements above with propane burner continiously activated.						

Measurements 1,2,5,7 and 9 are measurements where an increasing flow rate was supplied to the flare. This was done by increasing the pressure in the hydrogen buffer for higher flow rates and increasing the open position of the valve. Finally, an average flow rate of 6200 Nm^3/h was achieved during test 10 for 10 seconds. These are discussed in more detail in section 4.3.

Measurements 3, 4 and 8 were performed by draining the hydrogen buffer almost completely. This involved no (or limited) supply from the cylinder packs. In terms of visible flame size, sound and heat radiation, the flame became smaller and smaller. The flame continued to burn and showed no flash back. Because of the limited time, after a while, the valve was slowly closed. This accelerated the process of extinction. The course of heat radiation from measurement 4 is shown in Figure 11. Here, the hydrogen buffer was filled at 8 bar after which it depressurised via the flare in almost 10 minutes.

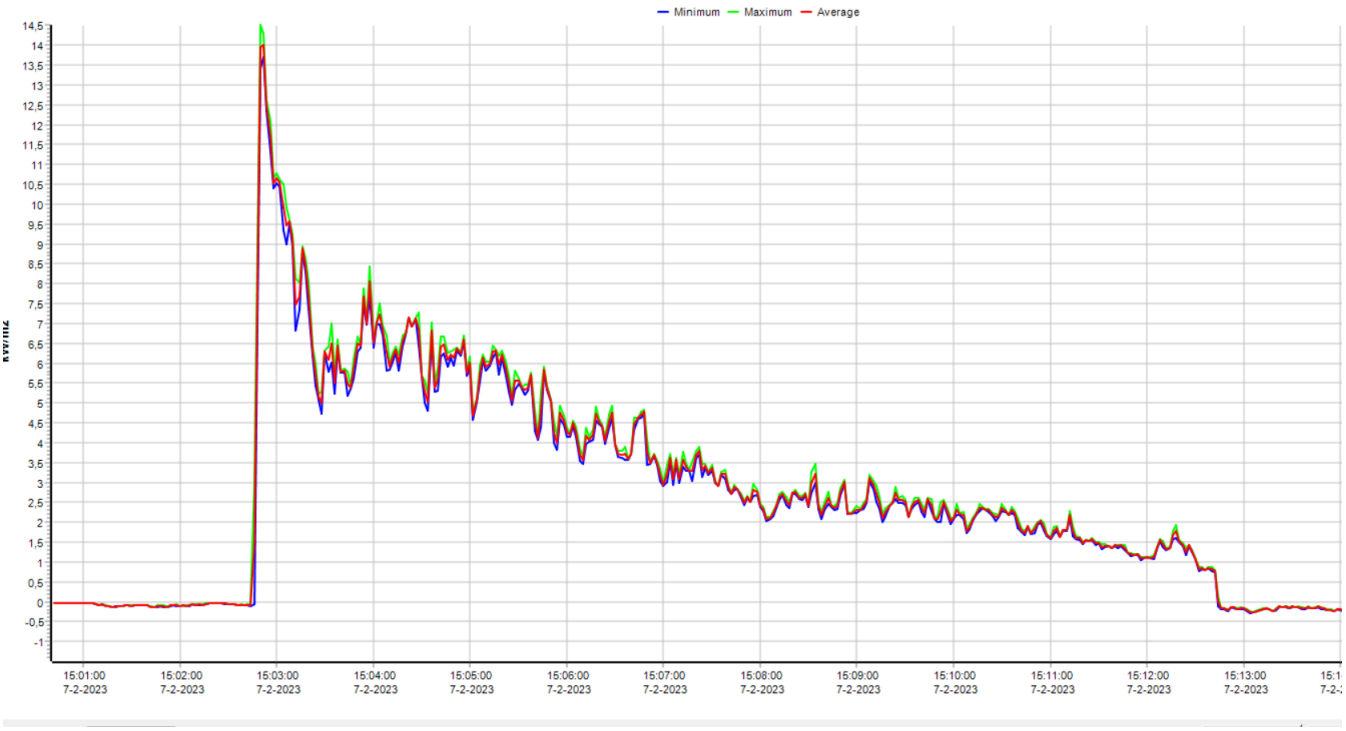

Figure 11: Heat radiation from an extinguishing flame (measurement number 4).

Around time 15:12:30, the valve is slowly closed. After this, the measured thermal radiation drops to 0. During these measurements, noise and NOx emissions were also recorded. See sections 4.4 and 4.5 for these details.

4.2 Delayed ignition

For the delayed ignition tests, the flare's built-in propane burner was turned off and the hydrogen mixture was ignited with a spark igniter placed just above the outlet. For the tests, the pipe section was filled to a certain pressure (4 or 8 bar). After this, the valve was opened and a certain period of time was waited (5, 10 or 20 seconds) after which the spark igniter was activated.
It is remarkable that during most tests, the flame front propagated in all directions just after ignition. Thus, the flame also propagated downwards, something not taken into account beforehand.

A total of 7 measurement series were carried out in which the flow rate and the time at which the ignition was activated were the variables. Each measurement series consisted of several separate measurements. During the different measurements, the time of ignition, noise level, wind speed and contours of the flame were recorded. Below is a summary of the measurements taken.

Table 4: Delayed ignition measurements performed

Series	Flow rate (global) (Nm^3/h)	Moment of ignition	Pressure in the buffer (bar)	Number of individual measurements	Comments
A	250	Spark present before gas supply was opened	4	6	Reference measurements - A large variation in the time of ignition observed. Sometimes 2 sec and sometimes 24 sec after opening gas supply.
B	250	10 s after opening gas supply	4	5	Again, a large variation in the timing of ignition observed. Sometimes 12 sec and sometimes 32 sec after opening gas supply.
C	250	20 s after opening gas supply	4	6	Again, a large variation in the timing of ignition observed. Sometimes 21 sec and sometimes 36 sec after opening gas supply.
D	3200	Spark present before gas supply was opened	8	7	Reference measurements after modification of spark igniters
E	1900	5 s after opening gas supply	4	4	Within 1 second of application of spark, ignition of gas
F	1900	10 s after opening gas supply	4	2	Within 1 second of application of spark, ignition of gas
G	3200	5 s after opening gas supply	8	4	Within 1 second of application of spark, ignition of gas

Based on the results of measurement series A, it was thought that the wind present caused slower ignition. After completion of measurement series C, the spark igniter was assessed. It was found to work less powerfully compared to the start of measurement series A. The wiring was replaced.
In measurement series D, the spark was activated and then a large flow rate of hydrogen was fed to the flare. In the first measurement in that series, the hydrogen ignited immediately. Then twice it did not. Probably because the spark formation faltered. In any case, the failure to ignite was not caused by the mixture being outside flammability limits. This is because while shutting off the gas supply, there was also no ignition during those individual measurements. Subsequently in the same set-up, with the same igniters, three more ignitions of hydrogen were observed. At the end of measurement series D (after the last individual measurement), the spark igniter no longer worked. The igniter was then replaced. With this spark igniter and wiring, measurement series E, F and G were performed.
During measurement series B, C, E and G, a spark was activated after unburned gas flowed out for some time. Based on these measurements, it appears that hydrogen is not spontaneously ignited.
See annex 9.2 for a summary of the results of all individual delayed ignition trials.

Ignition of the hydrogen in measurement series E, F and G was immediate (within 1 second) in each case after activating the spark igniter. The noise peaks in the delayed ignitions are higher than in the direct ignitions (see also section 4.4). This will be caused by a larger cloud of unburned hydrogen/air mixture being ignited. This ignition is visualised through the images below.

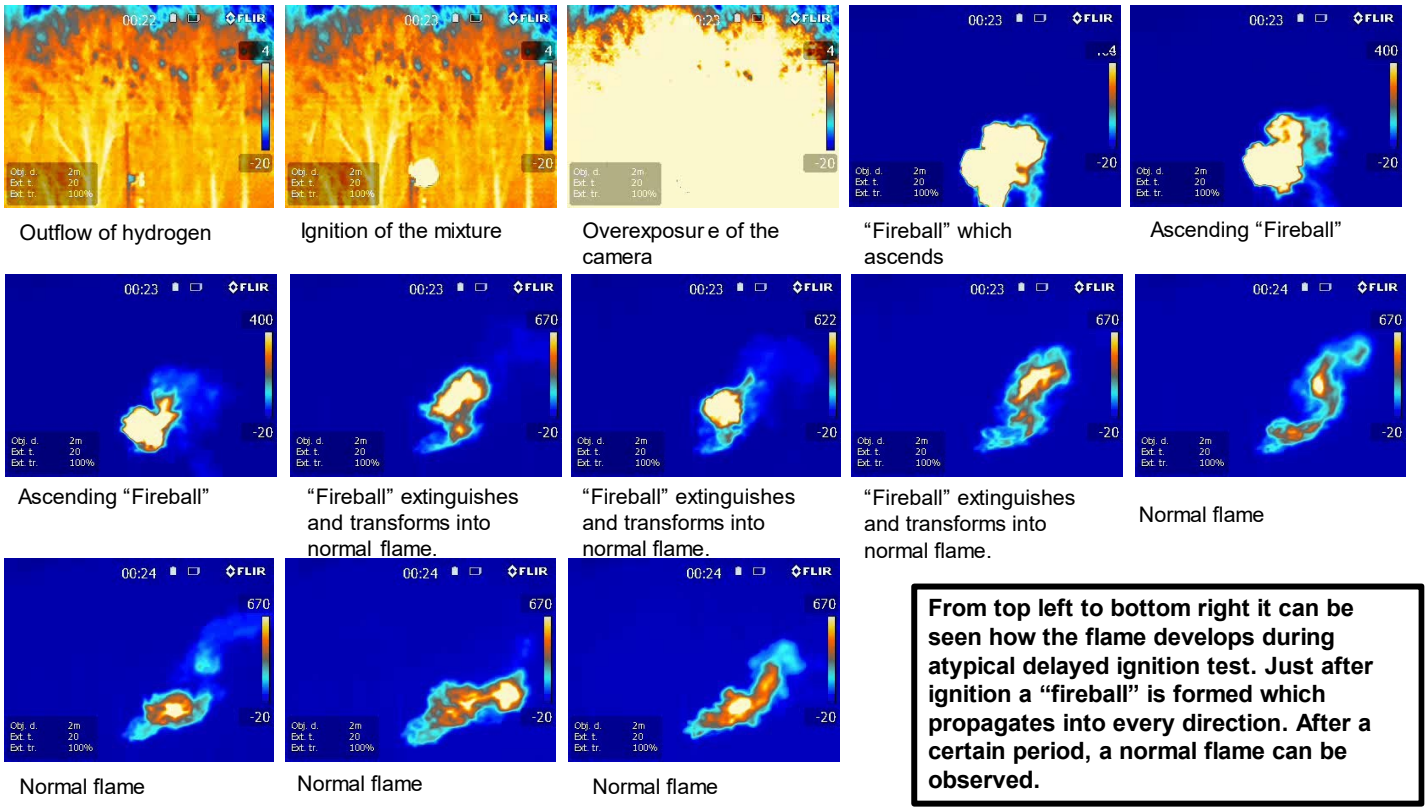

Figure 12: Images of a thermal imaging camera recording, from left to right represented increasing time.

The images from Figure 12 were taken at a delayed ignition test with a low flow rate (250 Nm^3/h). When the same delayed ignition is filmed with a normal camera, a lot less can be seen (Figure 13). It should be kept in mind that the comparison with the thermal imaging camera is difficult to make because the thermal camera gets overexposed during the build-up of the "fireball" and it has a lower capture rate (frames per second). However, the third picture in Figure 13 shows an orange glow around the flare. This is the "fireball" propagating in all directions just after ignition. For clarification, on the far right in Figure 13 the same photo is used again, with the contour of the "fireball" drawn in black. The whole process from ignition, creation of the fireball to its extinction and transition to a normal flame image takes 10 frames which corresponds to one third of a second.

Outflow of hydrogen | Ignition | "Fireball" | "Fireball"

Third picture where in black the contour of the flame is drawn. On the top right inside the contour, the hydrogen is not yet burning.

From left to right it can be seen how the flame develops during a typical delayed ignition test. After ignition, a "fireball" develops propagating into every direction. In this series of pictures, it can be seen how the "fireball" propagates. The "fireball" extends to approximately 0,8m below the flare exit. After a certain period, the "fireball" transforms into a normal flame.

Figure 13: Images from a video recording of delayed ignition.

4.3 Maximum flow rate testing

Due to the limited amount of hydrogen, as it had to be supplied by cylinder packs, two maximum flow tests were done. The test done last (9 February around 15:30) achieved the highest flow rate. The flow rate as a function of time is shown in the figure below. It can clearly be seen that the flow is highest at the beginning and decreases afterwards. The pressure in the spool (pipe section used as a buffer) is about 16 bar when the valve is opened. The pressure near the gauge shows a pressure of 13 bar just after opening. 10 seconds later, this has already dropped to 8 bar. From 30 s, a steady state follows until about 70 seconds. During this period, the pressure near the gauge is between 4 and 3.5 bar. After 80 seconds, the whole measurement is over.

The highest calculated flow rate was about 7000 Nm^3/h, however, given the run-in phenomena of the gas meter, it might have been a bit higher in the first seconds. In addition, in the first seconds there is a relatively large inaccuracy in reading the pressure gauge, it moves quite fast relative to the shutter speed. By combining and averaging the measurements of the first 10 seconds, it can be said with a high degree of certainty that a flow rate of 6200 Nm^3/h was achieved.

During testing, it could be observed that the flame was immediately ignited by the propane flame. This while the valve was fully opened within 10 seconds.

Since it is a dynamic process where the buffer is emptied and then refilled as best as possible by the cylinder packs which decreased in temperature, the flow rate steadily ran down after the first 10 seconds. After this, the flow rate stabilised around 2500 Nm^3/h which seems to be the maximum deliverable flow rate of the pressure regulators at these conditions.

The high-flow measurements included filming with the FLIR camera. Unfortunately, some thermal imaging camera recordings failed. As a result, only the first minute and a half of measurement 8 was filmed with the thermal imaging camera. This has a slightly lower flow rate than measurement 9, but is comparable at the beginning because the same 16-bar starting pressure was used.

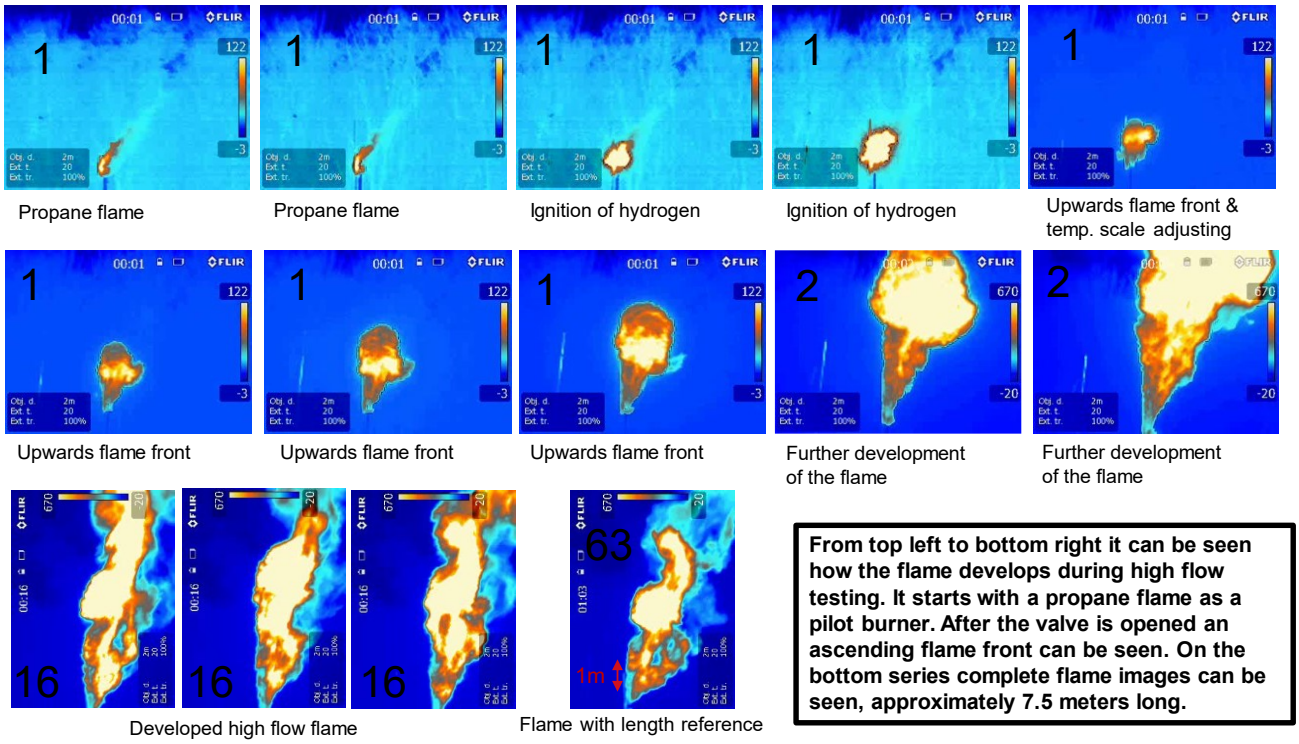

Figure 14: The course of a high-flow measurement captured by a thermal imaging camera. The numbers in black is the timestamp in seconds.

In the first second (the first 8 images) of the shot, the propane burner can be clearly seen (images 1 and 2). With this, the hydrogen flame becomes visible which can be seen from image 3 onwards. After this, the flame front moves upwards and also widens. After this, the camera is shifted and rotated a quarter turn to get a better view of the entire flame. The bottom left shows three images of a fully developed flame at 16 seconds. The flame height here is about 7.5m. This is derived from the last image (number 14), which was taken after 63 seconds. Here the flame is a lot smaller because the pressure in the spool has then decreased. In this image, you can clearly see the intake tube of the NOx sensor (red arrow). This is 1m long, and can be compared to the flame length of images 11, 12 and 13. In the experiment below (measurement 9, 6200 Nm³/h), this tube is moved to the other side (right in

Figure 14) shifted so that it draws in more combustion gases.

The thermal radiation in the high-flow tests is shown in Figure 15 and Figure 16. Here the correlation between pressure and thermal radiation can be seen, with thermal radiation appearing to lag slightly behind decreasing pressure.

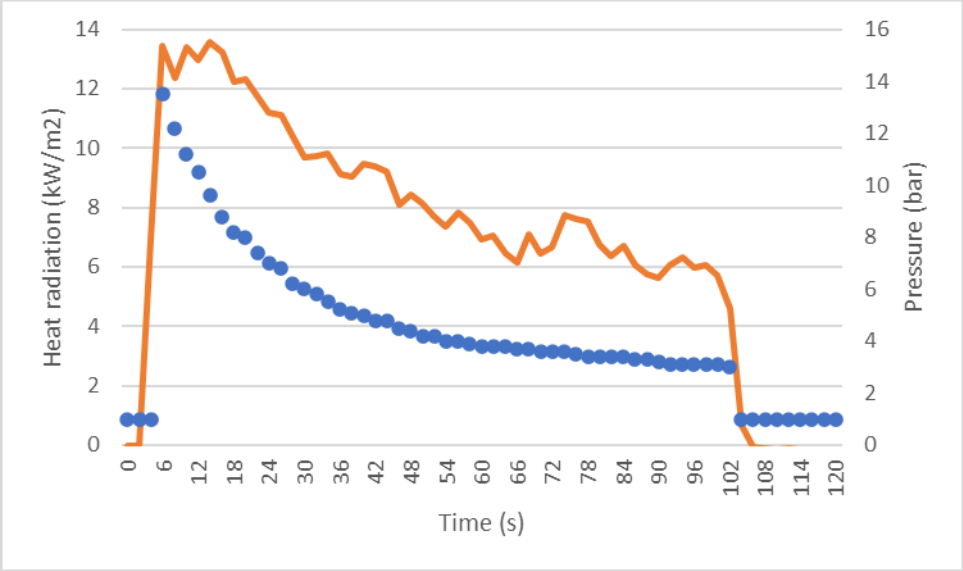

Figure 15: Heat radiation (red) and pressure at the gas meter (blue) as a function of time. (measurement 10)

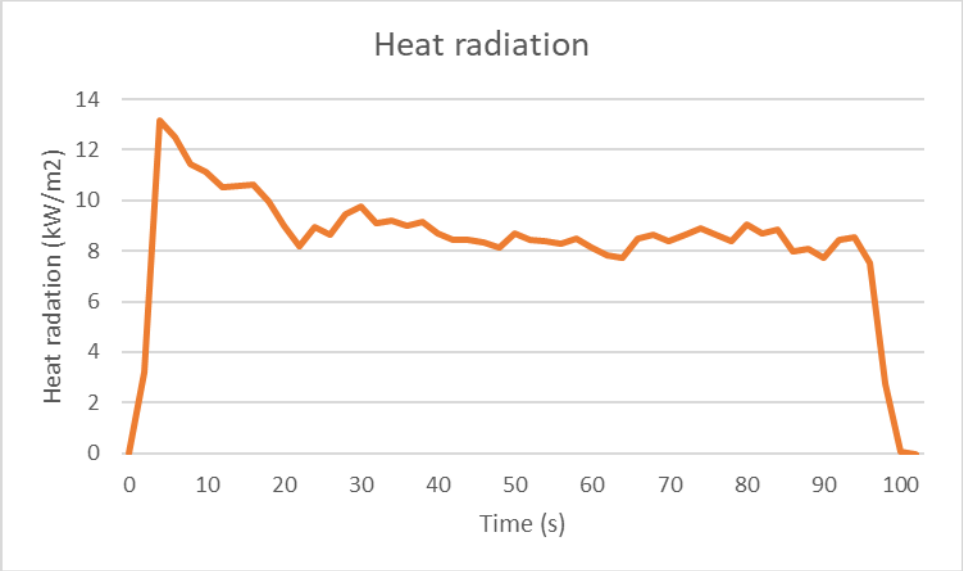

Figure 16: Heat radiation (red) as a function of time. (measurement 9)

During these measurements, noise and NOx emissions were also recorded. See sections 4.4 and 4.5 for the results.

4.4 Noise measurements

Noise measurements were made in all experiments. In this section, these are explained with a breakdown by direct and delayed ignitions.

4.4.1 Results sound measurements direct ignitions

The highest noise levels (measured at a distance of 3 metres from the flare and at a height of 1.5 metres above ground level) occur during hydrogen ignition. As stated in section 3.3.3 the LC peak values include all frequencies. The LAF max values do not consider the lowest and highest frequencies. These frequencies are not audible at noise levels <100 dB. After the hydrogen is ignited once, the noise level decreases. This can be seen in the value for LA eq. This represents an average noise level over the entire noise measurement. It should be noted that the noise measurement generally lasted longer than the period of ignition and combustion of hydrogen. The averaging in the form of LA eq therefore includes a period when the flare was not burning.
Based on the values LAF max at measurements 1, 5, 7 and 10, it can be stated that the noise level of a burning hydrogen flare has a noise level below 100 dB. The noise level of 100 dB is comparable to the noise of a circular saw.
The highest values for LA eq were observed at measurements 2 and 4 . The difference of the value LA eq between measurement 2 (84.0 dBA) and measurement 4 (85.1 dBA) is limited. This is despite the fact that in measurement 4 there was a hydrogen flame present during the entire noise measurement and in measurement 2 only half of the noise measurement.
The highest values for LC peak were observed at measurements 2 and 4 and not at the ignitions of the largest flow rate (measurements 9 and 10). At measurements 2 and 4, the gas concentration of hydrogen in the cloud with air is apparently closer to the stoichiometric ratio (30%) compared to the measurements with the maximum achievable flow rate.

Table 5: Results of noise measurements direct ignition

Meas. No.	Description	Flow rate (avg) (Nm3/h)	Noise			Time (sec)	
			LAF max (dBA)	LC peak (dB)	LA eq (dBA)	geluidsmeting	vlam
1	Experiment with low flow rate	680	98,8	125,0	68,7	180	120
2	Experiment with low flow rate	780	113,7	139,5	84,0	129	60
3	Emptying buffer, examination flashback	n.b.	106,8	131,9	77,9	130	90
4	Full spool, slowely burning to empty spool, at the end 2nd examination on flash back	n.b.	116,3	142,1	85,1	180	480
5	Increase of flowe rate by increase spool pressure	2500	94,6	123,2	74,8	187	150
6	Increase of flowrate, incorrect measurement related to determination of flow rate	n.b.	97,6	121,7	76,6	180	90
7	Increase of flowe rate by increase spool pressure	3750	93,0	120,9	80,1	160	100
8	Full spool, slowely burning to empty spool, at the end 3rd examination on flash back	n.b.	93,9	121,2	71,2	180	690
9	Maximum feasible flow rate in this set-up	n.b.	96,9	126,1	81,0	180	90
10	Maximum feasible flow rate in this set-up	6200	94,0	119,4	81,1	180	90
Alle measurements above with propane burner continiously activated.							

4.4.2 Results sound measurements delayed ignitions

The full results of the noise measurements are given in Appendix 8.2.

The noise peaks for the delayed ignitions of the higher flow rates (1900 and 3200 Nm^3/h) are higher than for the direct ignitions of the higher flow rates (2500, 3750 and 6200 Nm^3/h). This will be caused by igniting a larger cloud of unburned hydrogen/air mixture. The noise peaks at delayed ignitions of the lower flow rates (250 Nm^3/h) are around 130 dB. At direct ignition of a flow rate of 680 Nm^3/h, an LC peak value of 125 dB was measured and at a flow rate of 780 Nm^3/h, an LC peak value of 139.5 dB was measured. Because the low flow rates at the delayed ignitions differ from the low flow rates as measured at the delayed ignitions, a mutual comparison cannot be made properly.

Table 6: Maximum values for LC peak in delayed ignitions

Measurement series	Concerns individual measurement no.	Q overall (Nm^3/h)	LC peak (dB)	Moment of ignition activation
B	1	250	130,5	10 sec after opening gas / ignition 20 sec after gas release
C	6	250	131,0	20 sec after opening gas / ignition 27 sec after gas release
E	4	1900	139,8	5 sec after opening gas / ignition ~ 6 sec after gas release
F	2	1900	>143,9*	10 sec after opening gas / ignition ~ 11 sec after gas release
G	1 and 2	3200	>143,9*	5 sec after opening gas / ignition ~ 6 sec after gas release
G	3 and 4	3200	137,4	5 sec after opening gas / ignition ~ 6 sec after gas release
*143.9 dB is the maximum of the meter. In measurement 1 and 2 from Series G, the noise meter was placed 3 metres from the source, while in measurement 3 and 4 from Series G, the noise meter was placed 6 metres from the source.				

4.5 NOx emissions measurements

NOx emissions were measured in the direct ignition experiments. In this section a representation of the results as obtained from the direct ignition (section 4.1) and maximum flow rate (section 4.3) experiments.

As mentioned earlier, the flue gas intake opening is placed 1 metre above the flare. At the moment the propane burner is ignited, the propane burner's flue gases do not reach the measurement opening. It is conceivable that the propane burner's flue gases are carried along with the hydrogen flame. The flow rate of flue gases from the propane burner is of minor importance compared to the flow rate of flue gases from the hydrogen flame.
When the hydrogen is ignited, the suction opening of the NOx measurement point is located in the hydrogen flame at the time of almost windless conditions. As soon as the wind increases, the position of the measurement tube in relation to the chalice determines whether or not flue gases are sucked in. At flow rates 680, 780, 3750 and 6200 Nm^3/h, and the wind conditions prevailing at the time, NOx emissions could be determined. These are shown below.

This shows both the measured NOx emissions and the NOx emissions free of air. The latter is calculated based on the oxygen content also shown in the graph. Naming NOx air-free corrects for the dilution with air that takes place.

Table 7: NOx emissions measured at different flow rates

Measurement	Flow rate (Nm^3/h)	Wind speed (m/s)	NOx - max (ppm)	NOx - 0% O_2 max (ppm)	Time duration Hydrogen flame (s)	Measuring tube in flame
1	680	0,2	98	320	120	Yes, block of 50 s
2	780	0,3	80	206	60	0 to 20 s only
7	3750	0,6	262	275	100	Yes, block of 60 s
10	6200	0,3	807	848	90	Yes

Based on this limited number of measurement points, a correlation between NOx emissions and hydrogen flow rate can be seen.

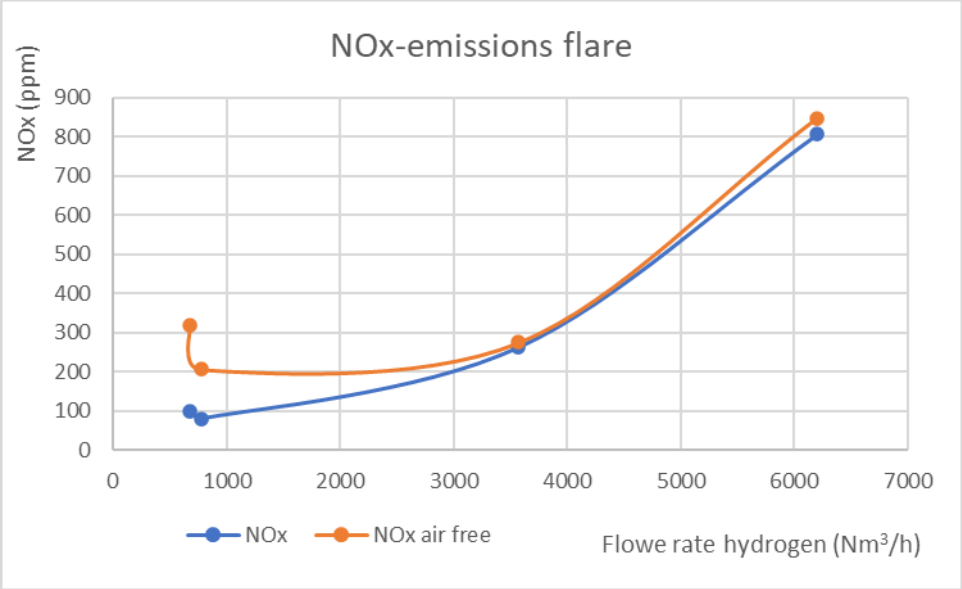

Figure 17: Increase in NOx concentration with increasing flow rate of hydrogen

At the lower flow rates (smaller than 1000 Nm^3/h), the difference between the measured NOx emissions and the calculated NOx emissions at 0% oxygen is large. This is because at these flow rates the oxygen content in the flue gases was high (>9%).
It should be noted that these NOx results provide an indication. For a proper NOx measurements all the flue gasses need to be captured and (a known part) should be analysed. This was not feasible in the in-situ conditions in which the experiments took place.

In Annex 9.1 the NOx emissions during flaring during measurements 1, 2, 7 and 10 are shown graphically, with the emissions fluctuating over the duration of the measurement. In that annex also the NOx emissions from the other measurements with direct ignition of the hydrogen flame.

4.6 Conclusions from the experimental studies

With the flare installation used, including flame arrestor, flaring flows in the order of 500, 2500, 4000 and 6000 Nm^3/h are feasible.

At a slowly decreasing gas flow rate, flame flashback does not occur. Whether the flame arrestor was necessary to prevent this has not been determined.

There is no excessive noise production during regular flaring, even when the hydrogen cloud is delayed ignited. During the tests with delayed ignition, there was, of course, outflow of unburned hydrogen gas. These flow rates, namely 250, 1900 and 3200 Nm^3/h, did not spontaneously ignite in the applied flare installation.

With increased hydrogen flow rate, the concentration of NOx in the flue gas increases. At the lowest flow rate tested (700 Nm^3/h) the measured NOx emission is about 100 ppm, at the highest flow rate tested (6000 Nm^3/h) the measured NOx emission is 800 ppm. At the higher hydrogen flow rates, the hydrogen/air mixture will be richer compared to the lower hydrogen flow rates. This may have been the cause of the higher NOx emissions. The higher NOx emissions may also be explained by the fact that the cloud of flue gases was larger and therefore less diluted compared to the measurements at low flow rates.

The contours of the flame were captured with a thermal imaging camera so that they could be compared with the models. The heat radiation from the flame was also recorded, which peaked at 14 kW/m^2 at the highest flow rate, at a distance of 2m from the flame. This data is useful in establishing the safety distances to be used for such a flare installation.

In the instant and delayed ignitions, no pressure waves were observed by the four people present during testing.

5. Modelling hydrogen flaring

5.1 Goals of modelling

To analyse a flare system, the properties of the gas at the flare tip must be known. In particular, the characterisation of the jet is important. The flow profile in the entire flare system can be used to safely design the experimental setup. Different levels of simulation can be used to describe the flow of hydrogen from the hydrogen system to the final combustion at the flare tip.

To understand the flow profile of hydrogen to the flare tip, process simulations can be performed. Whether it is constant flare activity or occasional blow-off events, process simulations can be run to monitor gas properties and system capacity at any time. Some examples of such tools include Flarenet (International), Aspentech Flare System Analyzer, PROMAX, Schlumberger's Flaresim/Flaresim Green, or Schlumberger's OLGA.

Hydrogen release and its combustion can be modelled using dispersion and flame models. These are highly computationally efficient and are based on experimental data and associated theory. From these models, flame shape, aerodynamic and temperature profiles can be calculated. From these, other derived quantities such as thermal radiation and noise contours can be derived. The tools mentioned above usually include this functionality. An example is Sandia National Labs' HyRam+ [4]. HyRAM+ is a continuously expanding tool that conveniently incorporates and links various analytical models.

Computational Fluid Dynamics (CFD) can be used for specific designs or conditions beyond the scope of more conventional models, as described above. However, CFD simulations are very time-consuming for such applications, as the (i) conservation equations have to be solved in their full form, (ii) taking into account the different molecules participating in the process, a representation of the combustion reactions and (iii) a radiation model for more accurate predictions. Full CFD simulations were not considered in this study.

5.2 Application to experimental setup

5.2.1 Flow profile along pipes

As described in section 3.2, the setup consists of a hydrogen cylinder and the pipe line segment as a buffer, a transfer hose, a vertical flare column with a flame arrestor and the damper at the tip. The flare is modelled in Schlumberger's OLGA (2021.1.2) as four different pipe elements, including one horizontal section (transfer hose), two 1.5-metre vertical sections and one 0.25-metre vertical section (diffuser/damper). The pipes leading hydrogen to the tip have an inner diameter of 2" and the damper is modelled as a short piece with an inner diameter of 4". In addition, some elements were introduced:

- A virtual valve at the transition from the hose to the damper. This is a 2" valve with a discharge coefficient of 0.84. This valve is included to ensure that choking can occur at this transition if the pressure ratio requires it.
- A pressure drop element with a coefficient of friction of 1 at the transition from the flare to the damper.
- A pressure drop element with a coefficient of friction of 1 at the damper-to-environment transition.

- A virtual valve at the position of the flame arrestor. This valve is included so that critical flow (choking) can occur in the flame arrestor. The size is adjusted to obtain the desired pressure drop as specified by the manufacturer.

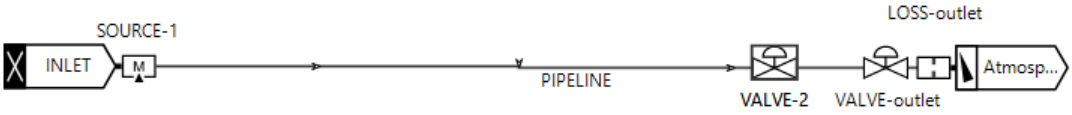

Figure 18: Overview of the OLGA model used to describe the flow profile to the flare in the experimental setup.

The modelling of the flame arrestor deserves special attention. The component KITO® FS-Def0-IIC used in the experiments has friction properties as shown in Figure 18. As can be seen in the figure, the maximum flow handled in this specification for size 2" reaches a maximum capacity of 60 Nm³/h (1 Nm³/min) and a pressure drop of 100 mbar. However, it is important to note that these values apply to air at normal conditions as the process gas. This should be translated to hydrogen. The supplier indicates that to use this chart for hydrogen, the values should be adjusted based on the following equation:

$$Q' = Q\sqrt{\frac{\rho}{1.293}}$$

where Q' is the value of flow rate [m³/min] to be used, Q is the actual expected flow rate for hydrogen [m³/min] and ρ the density of hydrogen at a given pressure. While this will be valid for most cases, it includes the implicit assumption that the Reynolds number is high enough not to observe second-order effects, and that the pressure drop is moderate. However, in the experimental conditions sought, the densities of hydrogen and air differ significantly, as does the pressure drop across the flame arrestor (with a limit value of 16 bar in the pressure regulators, which is considerably larger than the maximum value of 100 mbar that Figure 19 covers). Therefore, an alternative method is proposed in which the pressure drop is scaled according to:

$$\Delta P_{H2} = \Delta P_{air}\frac{\rho_{air}}{\rho_{H2}}\frac{\rho^2_{(n),H2}}{\rho^2_{(n),air}}\frac{Q^2_{(n),H2}}{Q^2_{(n),air}}$$

where ΔP represents the pressure drop [mbar] and ρ is the gas density [kg/m³]. The second method first requires the calculation of the pressure drop for the situation with air, so that the coefficient of friction at the highest flow rate can be used for the hydrogen situation.

The comparison between the two methods is given in Table 8 As expected, the methods hardly differ at low flow rates, but as conditions become more extreme, the alternative method gives significantly larger pressure drop across the flame arrestor at[3] .

The simulation results presented in this section follow the alternative method.

[3] The supplier was consulted directly on sizing the flame arrestor for the intended flows, and determined that a 5" component would be the optimal choice instead of 2". This does not mean that 2" is not possible, provided the system can accommodate the significantly higher pressures expected.

Table 8: Pressure drop calculated at the flame arrestor for 4 different hydrogen flow rates, according to the translation as indicated by the supplier or the alternative indirect method based on the data provided by the supplier.

	Direct translation manufacturer	Scaling from manufacturer data
H2 [Nm3/hr]	[pressure upstream [bara]	[pressure upstream [bara]
500	1.22	1.2
1000	1.44	1.7
2000	1.88	3.0
5000	3.21	7.0

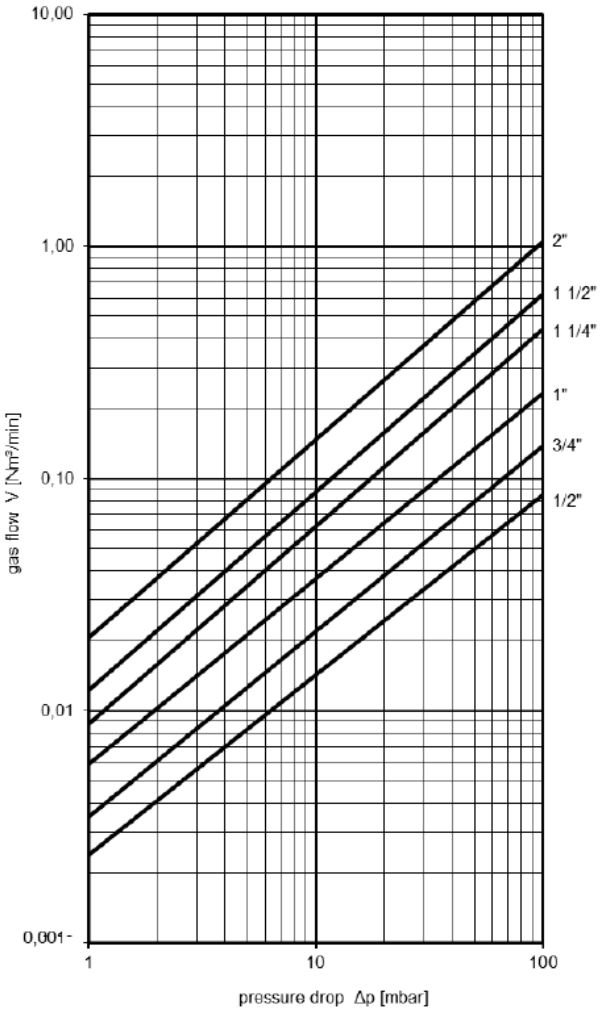

Figure 19: Pressure drop specification for KITO® FS-Def0-IIC. Assumes air at normal conditions.

The pressure profile and flow rate profile along the experimental setup for flow rates ranging from 500 to 5000 m³/h are shown in Figure 20 and Figure 21. For 5000 m³/h, the maximum upstream pressure is calculated to be ~7.7 bar(a) and a peak velocity of 600 m/s is calculated as the flow velocity upon entering the damper. In the experiments, pressure values around 7 bar(g) (i.e. ~8 bar(a)) are recorded. This indicates that the pressure drop in the flame damper is more consistent with the proposed alternative model and that the simulations are sufficiently reliable for all metrics related to hydrogen conditions upstream of the flare tip.

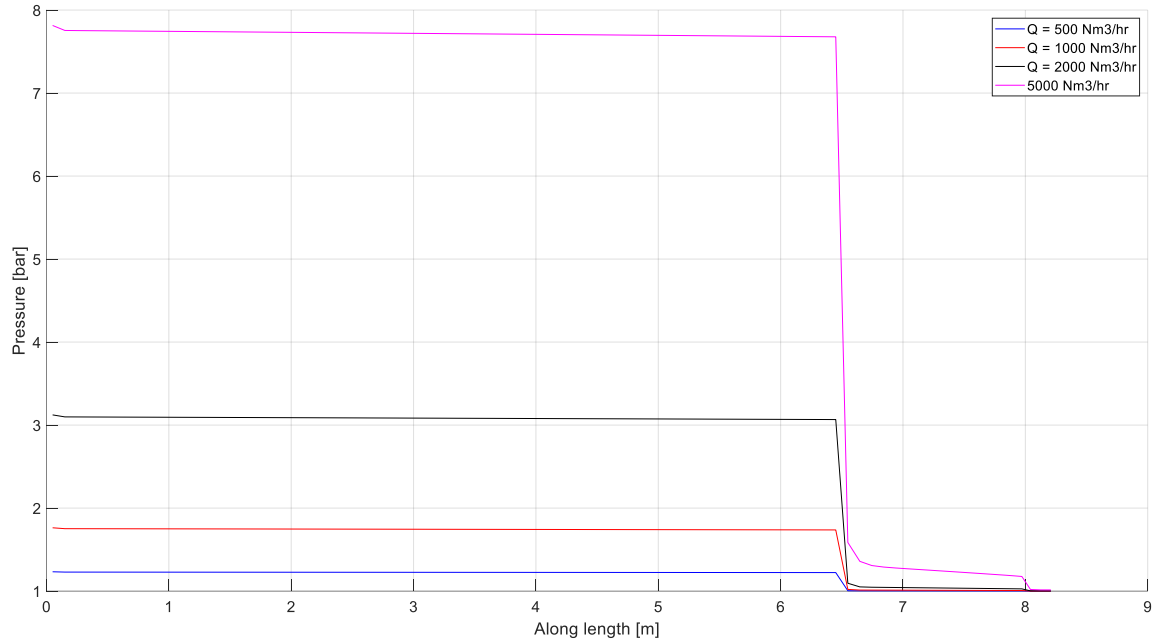

Figure 20: Pressure profile along the pipe line up to the flare tip.

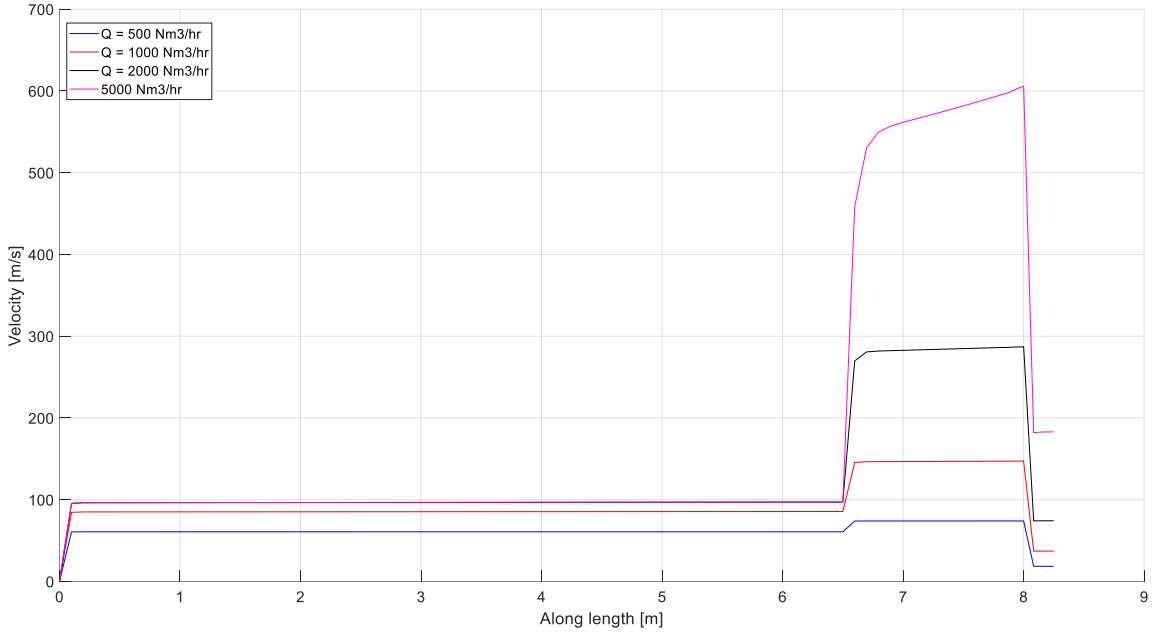

Figure 21: Gas velocity along the pipeline to the flare tip.

5.2.2 Description of the flame

It is important to know whether the flare functions as intended and no unignited hydrogen clouds are formed. As shown in the experiments, a hydrogen flame can be very difficult to see or even invisible during daylight conditions. Analytical models implemented in the HyRAM+ tool have been used for the experiments performed. HyRAM+ is a continuously expanding tool that conveniently incorporates and links different analytical models. The flame characterisation implemented in HyRAM+ is based on the work of Houf and Schefer [5]. The following assumptions were made when using the tool:

- Hydrogen is released from the flare tip at 2-inch and 4-inch diameter, due to the presence of the damper that makes the scenario more uncertain.
- No additional discharge coefficient (area correction) is applied.
- Wind conditions are neglected.
- The flow rate was tuned to a range of experimental values.

The calculated *visible* flame length is shown in Figure 22. Only at larger flow rates are there some small differences in the visible flame length between the 2" and 4" assumptions, due to a slightly different balance between the impulse of the jet and the buoyancy force. An example of the flame shape at 6000 Nm³/h (2") is shown in Figure 23. The model shows a very smooth, undisturbed flame geometry that does not take into account the generation of turbulence or wind gusts that disturb this shape.

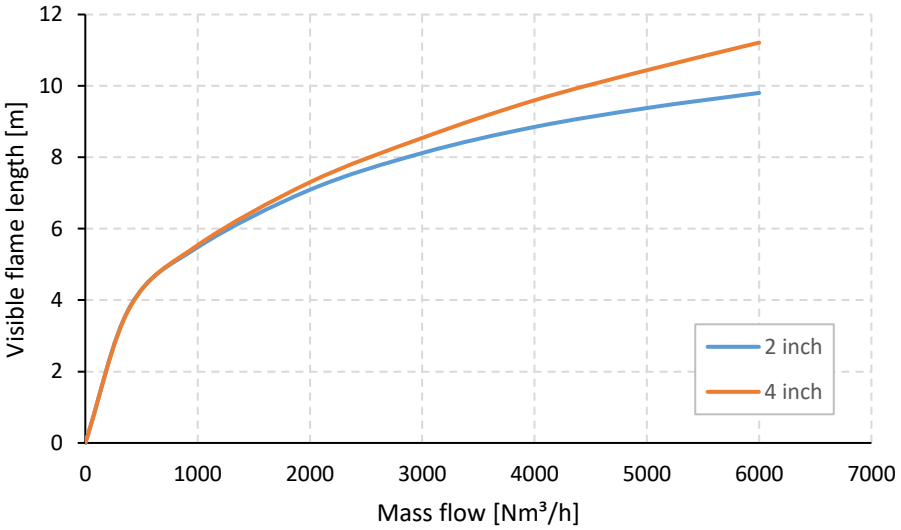

Figure 22: Calculated visible flame length as a function of mass flow rate of hydrogen from a 2" or 4" flare tip.

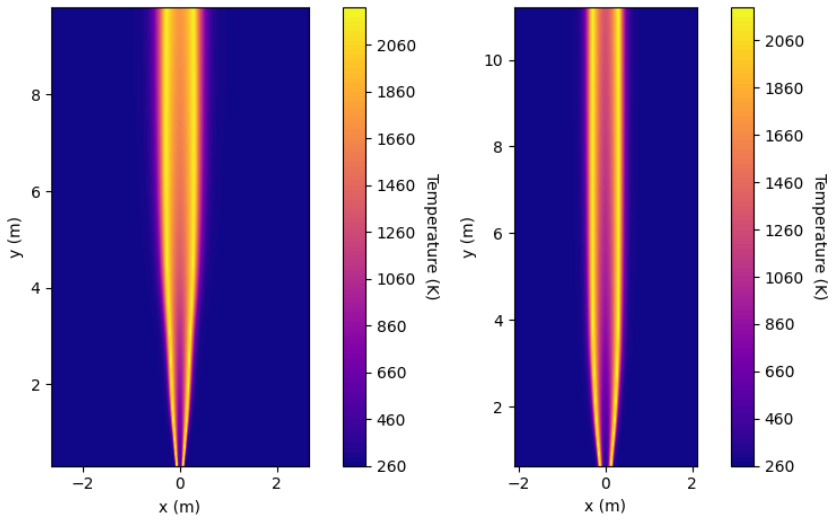

Figure 23: Calculated flame geometry. Left: clearance with a 2" opening; right: clearance with a 4" opening.

5.2.3 Heat radiation

The heat radiation from an open flame is very important for the safety of bystanders. The radiation power produced by an open flame is determined (linearly) by the heat of combustion of the fuel and the mass flow rate of the fuel, regulated by the radiation fraction. The radiation fraction depends on hydrogen-related properties and the description of the flame. Although the damage caused by thermal radiation to humans depends on both the magnitude and the exposure time, it is generally believed that a threshold of 1.58 kW/m² is safe[4] for continuous exposure.

The heat radiation contours were characterised for the conditions as measured in the experiments to determine the feasibility of using such tools for application in larger installations. Figure 24 shows the calculated values compared to the measured values. The calculations are performed at two radial distances in the plane 1 metre above the flare nozzle opening: 1 metre and 2 metres. The difference in the calculated values shows the sensitivity of the relative position between the receiver and the position of the flame. Wind conditions are not included in the calculations.

The results show reasonable agreement between calculations at 1 metre from the flare nozzle, with a maximum deviation of 20%, especially during the flow change. At flow rates around 2000-3000 Nm³/h, the measurements give a wide range of radiant heat fluxes between 6 and 10 kW/m², a variation assumed to be caused by wind gusts that change the position of the flame and thus the radiation at a fixed point. The total experiment takes about 80 seconds, of which about 40 seconds are in this flow range, with a possibility for wind to disturb these measurements.

At the maximum flow rate of 6000 Nm³/h, the safe distance from the flare tip is shown in Figure 25. This graph shows that a distance of about 10 metres is necessary to stay below the threshold value of 1.58 kW/m². In practice, because the stack is at a nominal height of 1.5 metres above the ground, the value can be reduced to about 8 metres. However, due to wind conditions, it is recommended to stay at distances > 10 metres.

Given the reasonable agreement between the calculations and experiments, it can be argued that the models embedded in the HyRAM tool can be useful to determine flame characteristics and safe distances when using actual mobile flares to degas segments of the high-pressure network.

[4] Pre-normative REsearch for Safe use of Liquid Hydrogen (PRESLHY) EIGA DOC 211/17 Table 3

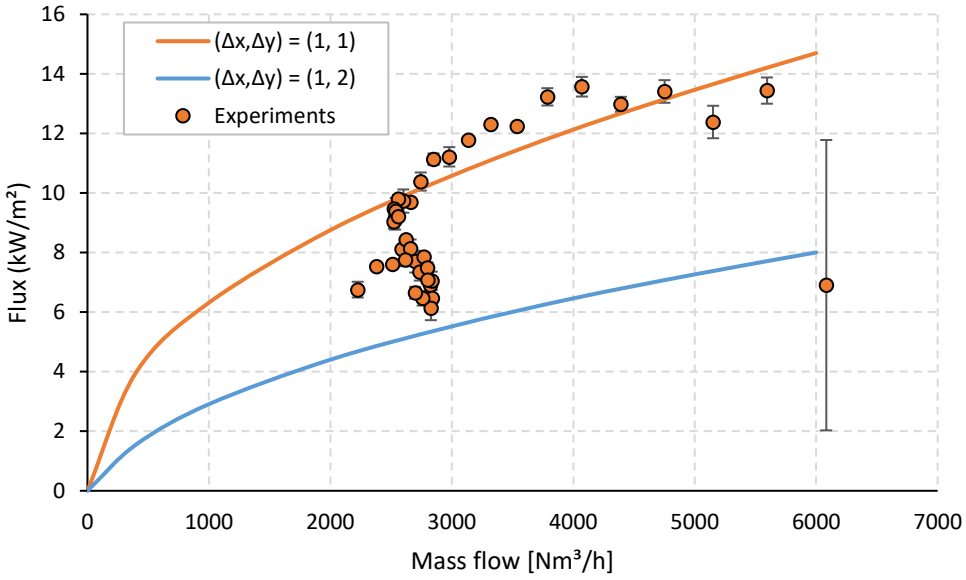

Figure 24: Calculated radiant heat flux [kW/m²] at two relative positions from the flare tip opening. The experimentally recorded values are given for comparison.

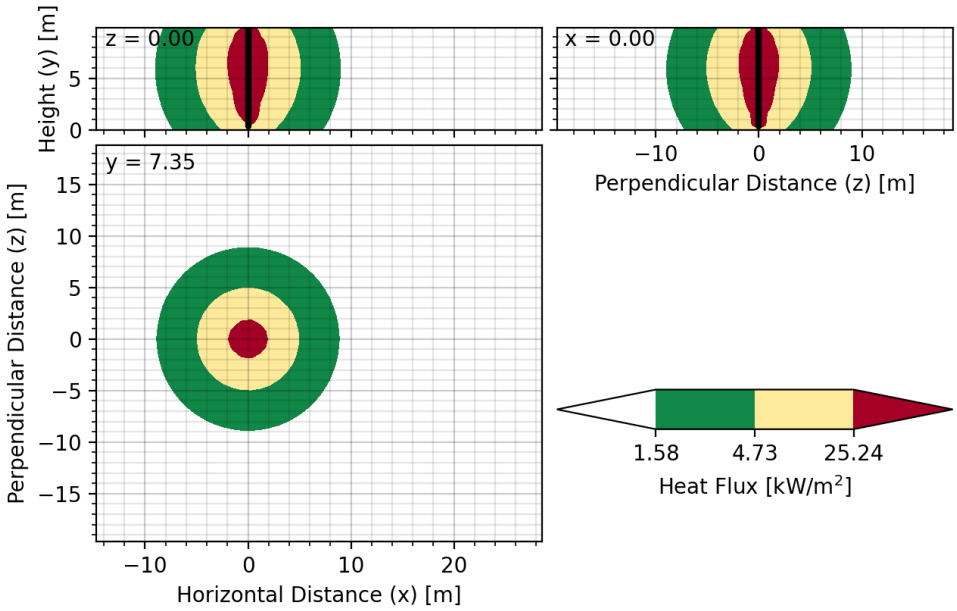

Figure 25: Safe distance calculated using the HyRAM tool, showing that a distance of about 10 metres from the vertical axis of the flare tip is necessary at flow rates of 6000 Nm³/h.

5.2.4 Sound

The sound of flaring is produced by several mechanisms, the most important being:

- Combustion noise
- Jet turbulence/mixture noise,

Despite the complexity of these noise-producing mechanisms, a number of models are available in the literature that can provide an estimate of the noise produced by a flare using a single equation. The models are briefly described in the following paragraph. Model predictions based on process conditions during the flare test are examined in subsequent sections.

Simple flare sound models

Reference [6] provides an initial overview of models that can be used to estimate flare noise, although more options are available.

The VDI 3272 [7] is the simplest method, and describes the total sound power level for an elevated (open) flare as

$$L_{WA} = 112 + 17\ log_{10}\left(\frac{Q}{Q_0}\right)$$

The model assumes a simple relationship between the sound power level L_{WA} (in dBA) and the total mass flow rate Q expressed in tonnes per hour (t/h). Parameter Q_0 is a reference value of 1 t/h. The model developed by Mueller-BBM is slightly more sophisticated:

$$W_{AC} = TAE \cdot a \cdot Q \cdot H$$

in which

W_{AC}	Acoustic sound power (W)
TAE	Thermo-acoustic efficiency (-)
α	Conversion constant, 0.293 W.hr/Btu
H	Heating value (Btu/lb)
Q	Mass flow (lb/h)

The BBM-Mueller model assumes that a constant fraction of the total energy in the flame zone is converted into sound. This is called the thermoacoustic efficiency (TAE). A wide range of possible values are reported for hydrocarbon flares, ranging from 10^{-6} to 10^{-9}[8].

Sabratha University has developed a model that estimates sound power levels from

$$W_{AC} = \frac{(K-1)\gamma Q^2 U_{FLAME}^2\, {}^{d}/_{V}}{4\pi\rho c}$$

in which

W_{AC}	Acoustic sound power (W)
K	Gas expansion ratio (-)
G	Stoichiometric air-fuel ratio (-)
Q	Mass flow (kg/s)
U_{FLAME}	Average flow velocity through the flame area (m/s)
d	Diameter flame area (m)
V	Volume of the flame area (m)^3
ρ	Density of air (kg/m)^3

c Speed of sound in air (m/s)

Application to tests

The models summarised above have been used to estimate the noise levels experienced during the flare tests. The following process conditions are assumed to be representative of those conditions.

Table 9: Overview of relevant parameters for the noise prediction models.

Symbol	Description	Value	Unit
r	Distance microphone to flare	6	m
T_0	Ambient temperature	288.15	K
p_0	Environmental pressure	1.015	bara
LHV	Lower heating value of hydrogen	120	MJ/kg
K	Expansion ratio	848	-
γ	Stoichiometric air-fuel ratio	0.029	-
ρ_{HN}	Density of hydrogen under normal conditions	0.0899	kg/m^3
ρ_{AN}	Density of air under normal conditions	1.2	Kg/m^3
c	Speed of sound in air	340	m/s

A field test was organised in which a fixed and pressurised volume of hydrogen was flared to the environment. The process can be represented as the emptying of a balloon, with the driving pressure and outflow velocity gradually decreasing as the volume is emptied. Because the flow rate changes over time (Figure 11), direct comparison with noise prediction models is more complicated. Information on process conditions and recorded noise at a given (constant) flow rate should be known, for which the process simulations were performed (section 5.2.1).

The data recorded on 9 February at 15:20 (measurement 9 as described in Table 3, label sound file 20230209_152057) will be used for comparison. The volume flow rate during this experiment is seen decreasing from 7020 Nm^3/h to about 2350 Nm^3/h within 94 seconds. The noise calculated at 7000 Nm^3/h and 2500 Nm^3/h will therefore be calculated using the noise models, with the aim of providing an upper and lower limit to the expected noise from the flare. These will then be compared with the average noise measured during the test.

During measurement 9, the distance from the microphone to the flare installation was set at 6 metres. The equivalent sound level $L_{A,eq}$ was measured as 81 dBA, although levels fluctuated between a maximum of 96.9 dBA (greatest flow rate) and 64.2 dBA (probably measured when there is no more flow).

Table 10: Noise ratios according to VDI 3272 for an elevated flare.

Flow rate[Nm³/h]	Sound pressure level at a distance of 6m [dBA]
7000	82
2500	73.9

Despite the simple approach in VDI 3272, the estimated sound pressure levels (in dBA) are of the right order of magnitude.

Table 11: Noise spectra according to the Mueller-BBM model, using an area of thermoacoustic efficiency.

Flow rate [Nm³/h]	Adopted TAE (-)	Sound pressure level at a distance of 6m [dBA]
2500	1e-4	62
	1e-5	52
	1e-6	42
7000	1e-4	67
	1e-5	57
	1e-6	47

The Mueller-BBM noise prediction model is easy to use because it assumes a linear relationship between the mass flow rate and the sound power. However, the Mueller-BBM model relies heavily on a given assumption for the thermoacoustic efficiency that can be used for the whole flare. This is generally not the case; for a given mass flow rate, the efficiency with which sound is created varies through the whole flame area. Moreover, the TAE depends on the mass flow rate. It is suspected that this contributes to the difference between the predicted noise level and the average sound pressure level.

Table 12: Noise spectra of the model developed by the University of Sabratha. Properties of the flame area taken from HyRAM simulations (4 inches).

Flow rate (Nm³/h)	Flame height (m)	d (m)	U_{FLAME} (m/s)	Sound pressure level at distance of 6m (dB)
2500	8	0.1016	85.7	81.0
7000	12	0.1016	239.8	94.1

Some of the results of the survey presented in section 5.2.2 HyRAM calculations reported have been used as inputs to the calculations. In particular, the height of the flare at the corresponding flow rate is used to calculate the average flow rate through the combustion zone via

$$U_{FLAME} = \frac{Q_m}{1/4\,\pi d^2 \rho}$$

where Q_m is the fuel mass flow rate (kg/s), d is the diameter of the basin containing the most hydrogen (m) and ρ is the density of hydrogen under prevailing conditions. As a first approximation, the value of d is set equal to the outlet diameter of 4 inches. This approach shows that the predictions of the model developed by Sabratha University are in reasonable agreement with the measured average equivalent noise level of 81 dBA.

It is important to note that it is not possible to directly compare sound pressure levels expressed in dBA with levels expressed in dB. Sound pressure levels expressed in dBA are frequency-weighted using an A-filter. A-weighting is a procedure in which the frequency content of a signal is weighted based on the perceived loudness of sounds perceived by the human ear. A-weighting gives more weight to frequencies in the middle range of the human audible range and less value to frequencies close to the edges. Conversion from dBA to linear dB and vice versa cannot therefore be done without knowledge of the spectral content (amplitude per frequency bin) of the signal in question. The values will generally agree if most acoustic energy is present between 700 and 10 kHz.

6. Conclusion, discussion and recommendations

6.1 Conclusions experimental research

With the utilised flare installation, flaring hydrogen with flow rates in the order of 500, 2500, 4000 and 6000 Nm^3/h have been demonstrated. At slowly decreasing flow rates, almost towards 0 Nm^3/h, no flame flashback was observed. Whether the built-in flame arrestor was necessary to prevent this has not been established.

There was no excessive noise production or perceptible pressure wave during the flaring experiments. No excesses in pressure or noise were observed during the delayed ignition tests up to 8 bar. During the delayed ignition tests, unburned hydrogen flowed out of the flare at a rate of 250, 1900 and 3200 Nm^3/h. During this outflow, the hydrogen did not ignite spontaneously, but required an external source to initiate the flame.

There is an indication that with increasing hydrogen flow rate, the concentration of NOx in the flue gas increases. At the lowest flow rate tested (700 Nm^3/h) the measured NOx emission is about 100 ppm, at the highest flow rate tested (6000 Nm^3/h) the measured NOx emission is 800 ppm.

The heat radiation from the flame was recorded by a heat radiation sensor, it peaked at 14 kW/m^2 at the highest flow rate at a distance of 2m from the flame. This data is useful in establishing the safety distances to be used for such a flare installation. In addition, the results of the thermal radiation sensor, combined with the flame contours captured by a thermal imaging camera, were used to compare the models with these empirical results.

6.2 Conclusions theoretical research

Modelling activities were carried out to make estimates of the flow profile during the tests to understand whether the models can be used for large-scale applications. A model of the test rig was built in OLGA and combustion at the flare was studied with HyRAM+. The following conclusions were obtained:

- Feedback from industry indicates that there is sufficient knowledge to design a flare suitable for hydrogen on a large scale. Existing models or technical standards can be used for this purpose. There may be opportunities to convert existing natural gas flares for hydrogen, although no strong statement was received on this. It was also noted that flaring is preferable compared to venting, to avoid uncontrolled ignitions and for environmental reasons. However, none of the suppliers consulted had applications of mobile flares for hydrogen service.
- Hydrogen will expand faster in a given volume compared to natural gas. For a given pressure and burner geometry, the resulting volume flow will be about 3 times higher compared to that of natural gas.
- The flame arrestor in the setup forms a choking point, so the mass flow rate is directly linked to the upstream pressure (the result of the pressure in the hydrogen cylinder and the pressure regulator set points). The pressure increases significantly when reaching high flow rates of almost 6000-7000 m^3/h. The model and experiments agreed very well. This should be considered when sizing large-scale plants.
- Ultimate flames at flow rates of 6000 m^3/h are calculated at about 10 metres height, with hot spot temperatures of about 2000 K. The total radiated power at maximum flow rates is more than 1 MW, with values reaching safe exposure levels (< 1.58 kW/m^2) at distances of

about 10 metres. The calculated values agree well with the measured levels at the measurement site.
- Noise levels can be estimated using different models based on different datasets. Reasonable agreement was found between the models and experiments (order of magnitude 80 dBA at a distance of 6 metres, with peaks above 90 dBA at maximum flow rates).

6.3 Discussions

In order to make pipeline sections hydrogen-free in case of work, first of all as much as possible buffering and recompression will have to take place so as not to waste hydrogen and to keep the environmental impact as low as possible. Once this recompression has taken place, in the case of the national network, the gas pressure will still be around 7 barg. This residual gas should be vented or flared.
The benefits of flaring are;
- No unwanted ignition can occur outside the flare; ignition takes place in a controlled manner
- The cloud containing hydrogen is limited
- The impact of hydrogen as a greenhouse gas has been eliminated.

The advantages of venting are;
- No NOx emissions occur
- The risk of flame flashback is more limited compared to flaring.
- No chance of burning components in the environment

Although no spontaneous ignition was observed during the experiments, several parties consulted unanimously and strongly recommended avoiding hydrogen cloud formation by flaring. This will also avoid the non-negligible greenhouse gas potential. It is therefore concluded that flaring is preferable to venting. For flaring in case of depressurisation of a hydrogen filled pipeline a flame arrestor is theoretically not necessary. After the pipeline section is depressurised, the pipeline section will have to be made hydrogen-free. This must be done with nitrogen in order to prevent the formation of a flammable mixture in the pipe section. After the work on the pipe section has been completed, it will have to be made airless again. This again by flushing with nitrogen and venting via the venting/flaring installation. If the pipeline volume is limited, the amount of nitrogen carried along with the hydrogen afterwards may be acceptable. If this is not the case, hydrogenate the closed pipe section by purging via the blow-off/flare installation until sufficient hydrogen is measured at the blow-off opening or until the hydrogen is ignited at the flare installation (continuous energised ignition). In the unlikely event that air did remain in the pipe section, it is advisable to apply a flame arrestor in the flare installation to be on the safe side.

It has not been investigated to what extent the results obtained in this study can be extrapolated to larger flow rates, diameters and pressures.

6.4 Recommendations

Flaring after recompression is preferable to venting after recompression. However, in the context of NOx emissions, it is advisable to follow up on the following recommendations.

- Assess to what extent emissions of NOx (order of magnitude 0 to 1000 ppm in the flue gas flow) during flaring are proportional in terms of environmental impact to the emission of hydrogen (100% of the flow rate) during blowdown.
- Conduct additional research into NOx emissions at flare installations when using both natural gas and hydrogen. During these comparative measurements, flue gases should be measured as much as possible with a large measuring spider.
- Get the market to design flare installations that reduce NOx emissions as much as possible. The measurements mentioned above can be supportive here. A limiting factor on NOx formation may be the limitation of the flaring flow rate.

It is recommended to check to what extent the results obtained can be extrapolated for application of flaring of larger flows and at larger diameters.

Industry interviews generally indicated that designing flares suitable for hydrogen is possible without additional research. This state of knowledge is also confirmed by the reasonable agreement between existing (publicly available) models and the experiments conducted. At the same time, mobile flares for hydrogen service are not yet commercially available. It is therefore recommended to hold a market consultation with specialised suppliers to create the conditions necessary for the development of commercial products in the medium term.

7. Answering research questions

1. What (industry) standards are there for blowdown/flaring?
   Several standards in both America and Europe contain guidelines on how a system should be depressurised and include hydrogen conditions.

2. Are hydrogen flare systems for sale?
   Yes, in the Netherlands these are supplied by Esders, among others.

3. What are the differences with natural gas in terms of blowdown and flaring?
   Several properties important for flaring differ between natural gas and hydrogen. In general, the low density of hydrogen at atmospheric conditions, as well as the properties of the flame, will change the shape and instability of the flame, with an increased risk of flashback. This needs to be solved (usually) with a flame arrestor. Hydrogen will burn invisibly in most cases, requiring the need for special flame monitoring devices (such as an IR camera). Hydrogen flames are also expected to make more noise. Hydrogen is more susceptible to self-ignition due to static electricity discharges upon release.

4. What are the principles of safety?
   To protect workers and the public from the presence of the flare, risks related to thermal radiation and noise exposure must be carefully considered. Exact limits are determined by local regulations. For permanent flares, enclosed designs are generally considered safer.

5. What is the thermal radiation of a flare for hydrogen?
   The thermal radiation of a flare can be estimated using existing models. In the experiments conducted with the highest flow rates (> 6000 Nm^3/h), the thermal radiation exceeded 1 MW.

6. What is the maximum pressure in the flare installation?
   The tests were carried out with a maximum pressure in the buffer pipe section of 16 bar. The maximum pressure at the gas meter in this was 13 bar. Since there is still some pressure loss in the hose between the meter and the flare, the maximum pressure at the flame arrestor will have been around 13 bar.

7. What happens to the burner? What will be the size of the flame?
   No change was observed on the outside of the flare plant. The size of the flame was recorded using a thermal imaging camera, the height of the flame was ± 7.5 metres at 6000 Nm/h^3

8. Can hydrogen be ignited at the different flow rates/outflow rates?
   Ignition of hydrogen by means of a propane burner was found to be possible at flow rates in the order of 500, 2500, 4000 and 6000 Nm^3/h .
   Ignition of hydrogen by spark ignition was found to be possible at flow rates in the order of 250, 2000 and 3000 Nm^3/h.

9. What is the effect of delayed ignition?
   Delayed ignition to 8 bar has slightly higher noise levels compared to hydrogen direct ignition. The noise peaks for direct ignition of flow rates 1900 and 3200 Nm^3/h are higher than the noise peaks for direct ignitions of 2500, 3750 and 6200 Nm^3/h. A clearer bang is audible and measurable. With delayed ignition, there is a larger cloud of unburned hydrogen/air mixture compared to direct ignition of an equal flow rate. That larger cloud burns after ignition in a short time, creating a larger pressure wave. The resulting flame in delayed ignition propagates not only upwards but also slightly downwards.

10. Can detonation occur with delayed ignition? (theoretical consideration)
    During detonation, the flame velocity rises above the speed of sound. This is accompanied by large pressure waves. At the amount, mixing ratio and ignition energy applied during regular flaring, the occurrence of detonation is unlikely, ref [10].

11. Can unwanted ignition occur when venting? (e.g. from electrical discharge or friction due to high speeds)
    During the experimental tests, unburned hydrogen flowed through the flare unit at flow rates of 250, 1900 and 3200 Nm^3/h. No spontaneous ignition occurred during these measurements. In the unlikely event that this does happen, this (delayed) ignition will lead to the creation of a fireball that slowly turns into a burning flare. This is stated on the basis of the results described in 4.2.

12. What are the effects of flaring if the pipeline is almost empty?
    The flare system, including the flame arrestor, quietly extinguished. No abnormal phenomena were observed.

13. What NOx emissions occur?
    At flow rates of 700 to 6000 Nm^3/h, NOx emissions (air-free) occur from 200 to 850 ppm.
    At present, there are no requirements for NOx emissions at flares fired by natural gas or hydrogen in the Netherlands. This is partly because it is a flare installation and partly because the gas being fired is of clean quality.
    Although the number of operating hours does not affect whether or not NOx requirements apply, flare plants as used by the national grid operator and regional grid operators are likely to operate less than 500 hours per plant per year. For this reason, setting criteria on NOx emissions is less obvious. It does make sense, however, to examine what NOx emissions occur at flare plants fired to natural gas. The 800 ppm NOx is on the hefty side. For this reason, it makes sense to investigate how NOx emissions can be reduced.

8. Literature

[1] R. Bruschi, D. Ercolani and E. Donati, "Long Distance Transport of Natural Gas by High Pressure Pipelines," in *16th World Petroleum Congress*, Calgary, 2000.

[2] R. G. Derwent, "Global warming potential (GWP) for hydrogen: Sensitivities, uncertainties and meta-analysis," *International Journal of Hydrogen Energy,* vol. 48, no. 22, pp. 8328-8341, 2023.

[3] S. Guidard, W. Kindzierski and N. Harper, "Heat Radiation from Flares," Science and Technology Branch Alberta Environment, ISBN 0-7785-1188-X, Edmonton, Alberta., 2000.

[4] S. Gersen, "Literature research on low NOx hydrogen burners and developing design rules for low NOx burners," HyDelta, 2023.

[5] B. D. Ehrhart, C. Sims, E. S. Hecht, B. B. Schroeder, K. M. Groth, J. T. Reynolds and G. W. Walkup, *HyRAM+ (Hydrogen Plus Other Alternative Fuels Risk Assessment Models), Version 4.1,* Sandia National Labs, 2022.

[6] W. Houf and R. Schefer, "Predicting radiative heat fluxes and flammability envelopes from unintended releases of hydrogen," *International Journal of Hydrogen Energy,* vol. 32, pp. 136-151, 2007.

[7] C.-C. a. E. S. Hantschk, "Prediction of noise emissions from industrial flares," *Journal of the Acoustical Society of America 123, no. 5: 3692,* 2008.

[8] Verein Deutscher Ingenieure, "VDI 3732, Standard noise levels of technical sound sources - Flares," 1992.

[9] C.-C. a. E. S. Hantschk, "Flares-noise prediction and thermo-acoustic efficiency," in *AFRC-JFRC 2004 Joint International Combustion Symposium*, 2004.

[10] S. Tretsiakova, "Dealing with hydrogen explosions," HyResponse.

[11] A. Arrigoni and L. Bravo-Diaz, "Hydrogen emissions from a hydrogen economy and their potential global warming impact," Joint Research Centre, European Commission, 2022.

[12] A. Abusaloua, S. Ruqaia, A. Abdulbasit and Z. Waleed, "Environmental Study of Gas Flare System".

9. Annexes

9.1 Graphs NOx emissions and other NOx measurement results

Below are the graphs of the NOX emissions at various flow rates where the measuring tube was in the flue gases over a longer period of time. The graphs show both the measured NOx emissions and the NOx emissions free of air. The latter was calculated based on the oxygen content also shown in the graph. Naming NOx air-free corrects for the dilution with air that takes place.

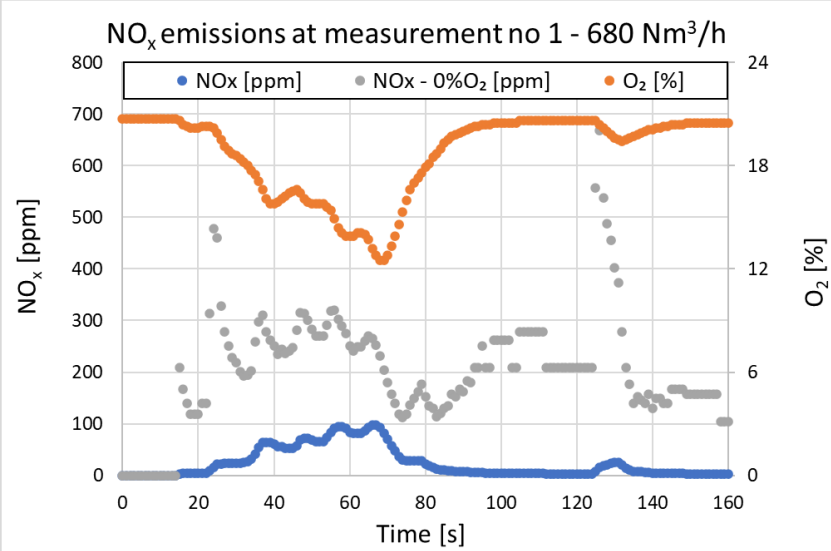

Figure 26: NOx measurements as a function of time (measurement 1)

The time duration of the hydrogen flame at measurement 1 was about 120 seconds. Over a period of 50 seconds, the intake of the measurement point was inside the flame. Where the NOx emission was low (<30 ppm) and the oxygen content was still high (>18%), the calculated NOx value at 0%O_2 was disregarded. The difference in reaction speed of NO sensors and O_2 sensors causes too much uncertainty in the calculated measurement value.

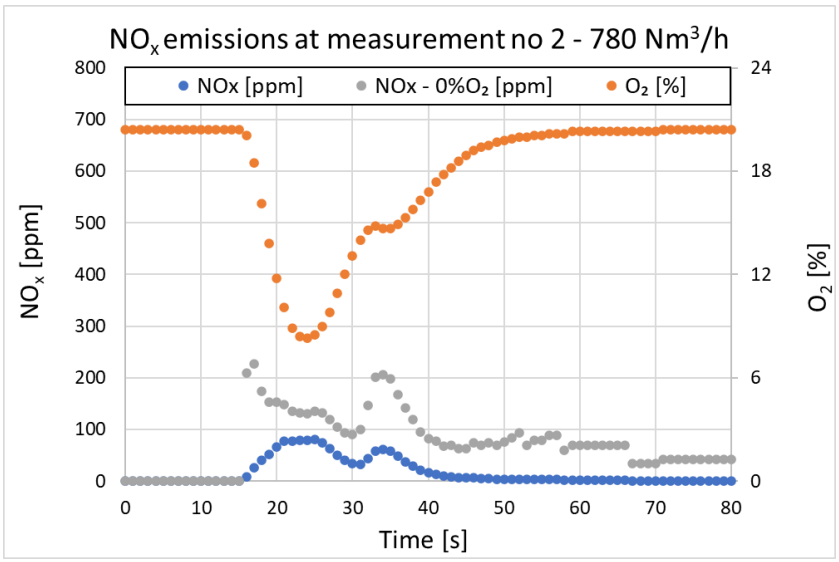

Figure 27: NOx measurements as a function of time (measurement 2)

The time duration of the hydrogen flame in measurement 2 was about 70 seconds. Only during the first part of the measurement, the intake of the measurement point was in the flame. Where the NOx emission was low (<30 ppm) and the oxygen content was still high (>18%), the calculated NOx value at 0%O2 was disregarded. The difference in reaction speed of NO sensors and O_2 sensors causes too much uncertainty in the calculated measurement value.

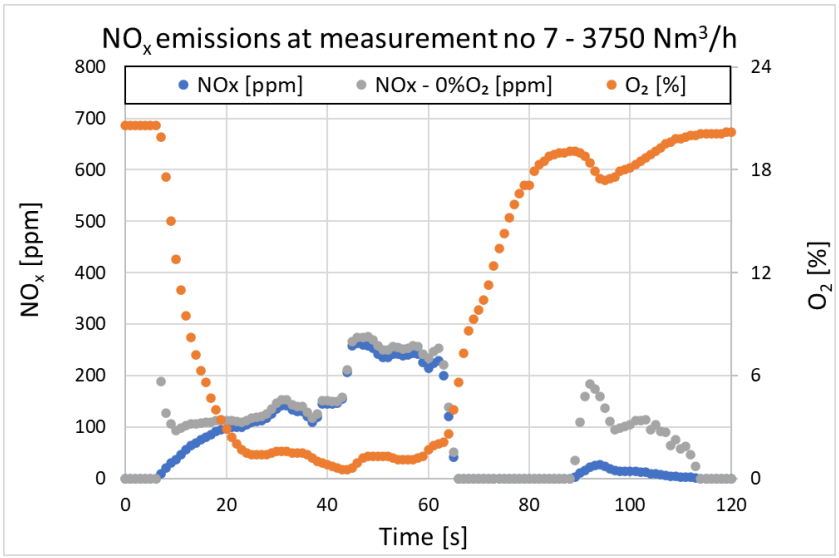

Figure 28: NOx measurements as a function of time (measurement 7)

The time duration of the hydrogen flame at measurement 7 was about 100 seconds. Over a period of 60 seconds, the intake of the measurement point was in the flame.

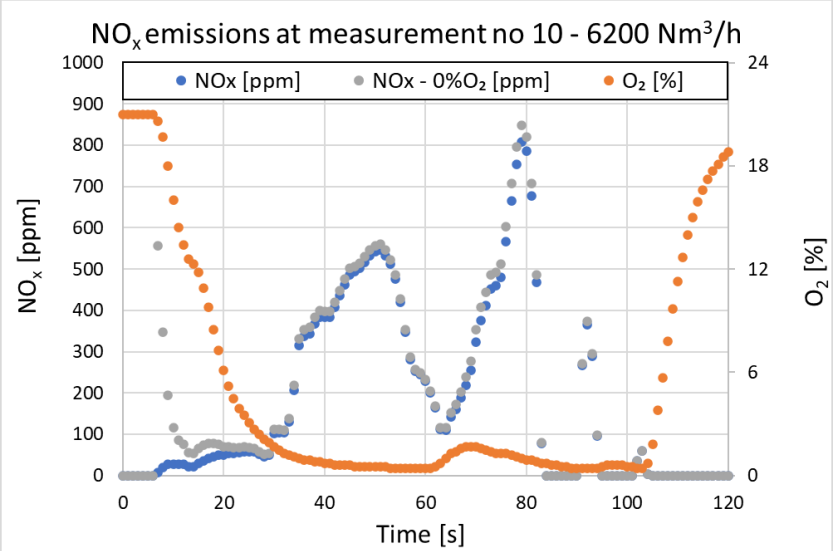

Figure 29: NOx measurements as a function of time (measurement 10)

The time duration of the hydrogen flame at measurement 10 was about 90 seconds. Almost the entire period, the suction nozzle of the measurement point was inside the flame.

Because in some measurements the measurement line was not or mostly not in the flame, not all measurements are usable. The not usable measurement results are shaded orange.

Table 13: Summary of NOx measurements in direct ignition tests

Meas. No.	Date	Description	Flow rate (avg) (Nm3/h)	Windspeed (m/s)	NOx - max (ppm)	NOx - 0%O_2 - max (ppm)	Meas tube NOX in flame?
1	06/02/2023	Experiment with low flow rate	680	0,2	98	320	yes, block of 50 s
2	06/02/2023	Experiment with low flow rate	780	0,3	80	206	yes, only first 20 s
3	07/02/2023	Emptying buffer, examination flashback	n.b.	0,4	30	n.d.	mostly not
4	07/02/2023	Full spool, slowely burning to empty spool, at the end 2nd examination on flash back	n.b.	0,4	52	n.d.	mostly not
5	07/02/2023	Increase of flowe rate by increase spool pressure	2500	0,8	0	n.d.	no
6	07/02/2023	Increase of flowrate, incorrect measurement related to determination of flow rate	n.b.	0,3	0	n.d.	no
7	07/02/2023	Increase of flowe rate by increase spool pressure	3750	0,6	262	275	yes, block of 60 s
8	07/02/2023	Full spool, slowely burning to empty spool, at the end 3rd examination on flash back	n.b.	0,5	23	n.d.	no
9	09/02/2023	Maximum feasible flow rate in this set-up	n.b.	0,6	2	n.d.	no
10	09/02/2023	Maximum feasible flow rate in this set-up	6200	0,3	807	848	yes (tube 180° moved)
Alle measurements above with propane burner continiously activated.					n.d. = not determined		

9.2 Moments of ignition and sound spikes delayed ignition

In the table below, for the different measurement series, as performed for the delayed ignitions, the moment of ignition of the hydrogen clouds are shown as well as peak noise values and the conditions under which these measurements were performed (flow rate and wind speed).

Table 14: Conducted measurement series and measurements in the context of delayed ignitions

Meetserie	Nr	Druk in leidingbuffer (bar)	Q globaal m^3n/h	Bekrachtiging ontsteker	Tijd tot ontsteking na openen gas (s)	LC peak (dB)	V wind (m/s)
A	1	4	250	Voorafgaand aan openen gas	1,4	-	1,8
A	2	4	250	Voorafgaand aan openen gas	24,0	-	1,7
A	3	4	250	Voorafgaand aan openen gas	2,6	131,0	0,9
A	4	4	250	Voorafgaand aan openen gas	13,4	130,3	1,6
A	5	4	250	Voorafgaand aan openen gas	1,8	132,3	0,5
A	6	4	250	Voorafgaand aan openen gas	2,1	128,5	1,2
Grote variatie in moment van ontsteking							
B	1	4	250	10 sec na openen gas	20,2	130,5	0,5
B	2	4	250	10 sec na openen gas	12,1	125,9	2,0
B	3	4	250	10 sec na openen gas	11,6	128,1	1,3
B	4	4	250	10 sec na openen gas	32,0	128,3	1,4
B	5	4	250	10 sec na openen gas	19,6	125,2	2,0
Grote variatie in moment van ontsteking							
C	1	4	250	20 sec na openen gas	31,5	122,3	1,7
C	2	4	250	20 sec na openen gas	34,2	129,1	1,1
C	3	4	250	20 sec na openen gas	20,9	<129,1	1,4
C	4	4	250	20 sec na openen gas	32,0	<129,1	0,9
C	5	4	250	20 sec na openen gas	35,5	129,5	1,3
C	6	4	250	20 sec na openen gas	27,0	131,0	1,0
Grote variatie in moment van ontsteking. Bedrading van de vonkontsteker vervangen.							
D	1	8	3200	Voorafgaand aan openen gas	<1	141	1,2
D	2	8	3200	Voorafgaand aan openen gas	geen		
D	3	8	3200	Voorafgaand aan openen gas	geen		
D	4	8	3200	Voorafgaand aan openen gas	<1	129,1	1,4
D	5	8	3200	Voorafgaand aan openen gas	<1	>143,9	
D	6	8	3200	Voorafgaand aan openen gas	<1	>143,9	1,3
D	7	8	3200	Voorafgaand aan openen gas	geen		
Na 7) vonkontsteker tikt wel, maar vonkt niet. Daarna is de vonkonsteker vervangen.							
E	1	4	1900	5 sec na openen gas	~ 6	139,4	0,6
E	2	4	1900	10 sec na openen gas	~11	136,6	0,0
E	3	4	1900	5 sec na openen gas	~ 6	132,9	0,6
E	4	4	1900	5 sec na openen gas	~ 6	139,8	0,9
F	1	4	1900	10 sec na openen gas	~11	140,6	1,8
F	2	4	1900	10 sec na openen gas	~11	>143,9	1,2
G	1	8	3200	5 sec na openen gas	~ 6	>143,9	1,0
G	2	8	3200	5 sec na openen gas	~ 6	>143,9	1,0
G	3	8	3200	5 sec na openen gas	~ 6	137,4	1,0
G	4	8	3200	5 sec na openen gas	~ 6	137,4	1,0
Na meting G2 de geluidsmeter verzet van 3 meter naar 6 meter vanaf de fakkel							
	de maximale waarde LC peak zoals weer te geven door de geluidsmeter is 143,9 dB						